Diploma Thesis

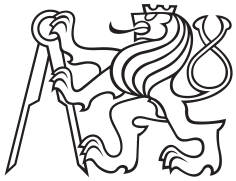

Czech Technical University in Prague

F4

Faculty of Nuclear Sciences and Physical Engineering
Department of Physics

Spectral analysis of quantum nanoribbons

Kateřina Zahradová

Supervisor: Mgr. David Krejčiřík, PhD., DSc.
Consultant: Ing. Tomáš Kalvoda, PhD.
Field of study: Mathematical Physics
May 2018

Acknowledgements

I would like to express my deepest gratitude to my supervisor David Krejčiřík for his time, patience, and invaluable advice throughout this year, as well as to my consultant Tomáš Kalvoda for all his help with computational and other computer issues.

My thanks also belong to my family and close ones for their unflagging support and love.

Prohlášení

Prohlašuji, že jsem svou diplomovou práci vypracovala samostatně a použila jsem pouze podklady (literaturu, projekty, SW, atd. . . .) uvedené v přiloženém seznamu.

Nemám závažný důvod proti použití tohoto školního díla ve smyslu § 60 Zákona č. 121/2000 Sb., o právu autorském, o právech souvisejících s právem autorským a o změně některých zákonů (autorský zákon).

V Praze, 4. května 2018

Abstract

The aim of this thesis is the generalization of several theorems about the spectral behaviour of the Laplace–Beltrami operator with Dirichlet boundary condition on quantum nanoribbons to arbitrary dimension as well as finding the spectrum of the (curved) Möbius strip. The notion of a quantum ribbon in an arbitrary dimension is introduced along with the proper definition of a quantum Hamiltonian for such strip. Theorems about the localization of essential spectrum for asymptotically flat strips, about bound states in purely bent strips and Hardy inequalities for twisted strips are presented. The spectrum of the Möbius strip is tackled in three different models both analytically and numerically, with comparisons of the results. We prove the norm–resolvent convergence in the thin strip limit for two of those models.

Keywords: nanoribbons, relatively parallel adapted frame, Möbius strip, effective Hamiltonian, twisting versus bending, bound states, Hardy inequality

Supervisor: Mgr. David Krejčiřík, PhD., DSc.

Abstrakt

Tato diplomová práce se zabývá zobecněním několika vět o spektru Laplace–Beltramiho operátoru s dirichletovskými hraničními podmínkami definovaného na kvantových nanostužkách v libovolné dimenzi, spolu s nalezením spektra pro Möbiův pásek. Definujeme pojem kvantového pásku v libovolné dimenzi a zavádíme na něm kvantový Hamiltonián. Věty o lokalizaci esenciálního spektra pro asymptoticky ploché pásky, o vázaných stavech v ohnutých páscích a Hardyho nerovnost pro zkroucené pásky jsou prezentovány. Otázka spektra Möbiova pásku je řešena pro jeho tři různé modely a to jak analyticky, tak numericky. Výsledky jsou pak vzájemně porovnány. Dokážeme, že v limitě tenkého pásku dva modely k sobě konvergují v norm–resolventním smyslu.

Klíčová slova: nanostužky, repér definovaný paralelním přenosem, Möbiův pásek, efektivní Hamiltonián, kroucení versus ohýbání, vázané stavy, Hardyho nerovnost

Překlad názvu: Spektrální analýza kvantových nanostužek

Contents

Introduction

Motivated by the study of transport in nano-structures, investigation of spectral properties of quantum waveguides dates as far back as to the beginning of the 1990's, with probably the first article being Exner and Šeba [16], quickly followed by many more (*e.g.* [7, 8, 15]). Subsequently, the spectra of different kinds of waveguides have been extensively studied – be it three–dimensional ones [21, 34], quantum layers [14, 13, 9], or quantum strips [2, 6, 32, 33]. Thorough investigation has not only focused on the Dirichlet Laplacian, rather both different boundary conditions, see *e.g.* [28, 11, 27] for the Neumann-Dirichlet or [19, 17, 36] for the Robin ones, and different operator settings have been examined, such as the magnetic Schrödinger operator in [5, 30].

Nevertheless, most of the known results only entertain the notion of a quantum waveguide in merely three dimensions. In this thesis, we wish to rectify at least a part of this by studying the spectral properties of nanoribbons in arbitrary dimensions. Let us stress here that the considered model consists of a strip (alias ribbon) and the Laplace–Beltrami operator defined on it, which differs from the other settings considered in the literature. This study is enabled by utilizing the generalization of the relatively parallel adapted frame, firstly introduced in 1975 [3] and generalised to higher dimensions in 2016 [40], for the definition of the strip. The main convenience of this choice is that said frame demands only very mild regularity assumptions on the curve and, moreover, these conditions do not depend on the dimension of the ambient space. This contrasts with the traditionally used Frenet frame, for which the regularity prerequisites quickly increase in higher dimensions. Therefore, by choosing the relatively parallel adapted frame as our tool for the definition of the investigated strips, we do not need to restrict ourselves with respect to the ambient dimensionality. This advantage is exploited in

Chapter 2, where we derive spectral results for asymptotically flat strips, confirm the manifestation of bound states in purely bent strips, and prove Hardy inequalities in twisted strips.

Not only have the higher dimensional examples of quantum waveguides been rather neglected in previous years, further, the elusive Möbius strip has been rebuffing most attempts on its spectral analysis. Even though the said strip has been extensively discussed in numerous settings, as far as the author is aware, its spectrum is yet to be determined. The closest work to the problem we tackle in Chapter 3 is Gravesen and Willatzen [22], where the effective model for a Dirichlet Laplacian defined on a thin tubular neighbourhood of the surface is studied. In contrast, we study only the two dimensional Laplace–Beltrami operator on the actual strip.

Possible division of the other examinations of the strip is to consider the material of the strip. Following this line of thought, we find that the rigid model was examined with respect to magnetization [20], movement of a free particle [22] or with respect to equilibrium shapes and stress localization [37]. The Möbius strip made out of graphene was considered in a number of papers – the electronic properties of a topological insulator with respect to the different edges [23], and the symmetries and their consequences for chemistry [18]. Furthermore, the lattice model is also popular – the square lattice Ising model was discussed [10], persistent currents of non-interacting electrons [39], or the problem of a continuous-time quantum walk on the Möbius lattice [35].

Another viable division is due to the ambient space in which the problem is treated. The former examples are all restricted to three dimensions, however, even generalizations to higher dimensions are being studied in various settings. The problem of the spectrum of numerous differential operators has been studied, *e.g.* [26] for the Klein–Gordon operator in $\mathbb{R}^n$ or [25] for the Helmholtz operator on higher dimension Möbius strip embedded in $\mathbb{R}^4$.

To summarise, the organisation of this thesis is as follows. The first chapter serves as a short introduction of the necessary facts, notions, and notations. The main results about the spectral properties of either asymptotically flat, purely bent or (purely) twisted waveguides are presented in the second chapter. The last chapter, Chapter 3, is devoted to the spectral study of the Möbius strip – we introduce three different models of said strip, the fake, the not–so–fake, and the full one, solve them analytically and/or numerically and, finally, present the result of norm–resolvent convergence of the latter two in the case of the width of the strip tending to zero.

Chapter 1

Preliminaries

This chapter is devoted to a brief recollection of several important concepts used throughout the thesis as well as to define certain new notions. In order to properly define quantum nanoribbons, the following ideas must be recalled first.

For the purpose of this thesis, we define a *curve* Γ in $\mathbb{R}^n$ as a mapping $\Gamma : I \to \mathbb{R}^n$ from any open interval $I := (a, b)$, where $a, b \in \mathbb{R} \cup \{-\infty, \infty\}$, into $\mathbb{R}^n$, which fulfils the following conditions:

- $\Gamma \in C^{1,1}$, *i.e.* Γ is continuously differentiable and its derivative, Γ', satisfy the Lipschitz condition:

$$(\exists C > 0)\,(\forall x, y \in I)\,\left(|\Gamma'(x) - \Gamma'(y)| \leq C|x - y|\right),$$

- Γ is regular, that is $\Gamma'(t) \neq 0$ for all $t \in I$.

The variable $s \in I$ is called *the parameter* of the curve. According to the classical result (*e.g.* [24]), every regular curve $\Gamma : I \to \mathbb{R}^n$ can be reparametrised in such a way, that $|\Gamma'| = 1$ on the whole interval I. From here on, by Γ' we mean the derivative with respect to the 'lengthwise' variable s, *i.e.* $\Gamma'(s) := \frac{\mathrm{d}}{\mathrm{d}s}\Gamma(s)$. Later on, the notation $\dot{\varphi}$ will be used to denote the derivative with respect to the transverse coordinate t. This special reparametrisation of the curve is called *the arc–length parametrization*. Curves parametrized by their arc–length are also called *unit speed* curves. As only regular curves are

considered here, it can be assumed without the loss of generality that they are already unit speed, so no reparametrisation is necessary.

A *moving frame*, or just *frame*, along the curve $\Gamma : I \to \mathbb{R}^n$ is a collection of n orthonormal differentiable vector fields $e_1, \ldots, e_n$, $e_i : I \to \mathbb{R}^n$ for $i = 1, \ldots, n$. It follows that the time evolution is given by a skew-symmetric matrix. The moving frame is called *adapted* if one of the vector fields coincides with the tangent Γ' of the curve. In such a case, all other components of the frame are normal to the curve. Another particular case of a moving frame is a *rotation minimizing frame*. Its time evolution fulfils that there exists an $i \in \{1, \ldots, n\}$ such that

$$e_j'(s) = k_j(s)e_i, \quad \forall j \neq i$$

for some functions $k_j : I \to \mathbb{R}$.

Since the relatively parallel adapted frame, which is used throughout this thesis, is solely a special case of the rotation minimizing frame, let us discuss its properties. The relatively parallel adapted frame, firstly introduced in only three dimensions by [3], is an example of an adapted frame minimizing rotation along its tangent. The main result of [40] generalises that and claims, that for every regular $C^{1,1}$ curve $\Gamma : I \to \mathbb{R}^{n+1}$ there exists a relatively parallel adapted frame. That is, for every regular $C^{1,1}$ curve in any dimension, there exists a frame consisting of $T, N_1, \ldots, N_n$ with time evolution given by

$$\begin{pmatrix} T \\ N_1 \\ \vdots \\ N_n \end{pmatrix}' = \begin{pmatrix} 0 & k_1 & \ldots & k_n \\ -k_1 & 0 & & \\ \vdots & & \ddots & \\ -k_n & & & 0 \end{pmatrix} \begin{pmatrix} T \\ N_1 \\ \vdots \\ N_n \end{pmatrix},$$

for some functions $k_i : I \to \mathbb{R}$, $i \in \{1, \ldots, n\}$. We call these *the parallel curvatures* and denote $k := (k_1, \ldots, k_n)$.

Now, let us proceed to the definition of a quantum nanoribbon. In order to do that, several auxiliary constructs have to be outlined first. Let ω be defined as $\omega := (-a, a)$ for some $a > 0$, $a \in \mathbb{R}$. Then ω is called *the cross section* and $\Omega_0 := I \times \omega$ is called *a straight strip* or *a straight ribbon*. To obtain an arbitrary one along our chosen curve Γ, one constructs the following mapping

$$\mathcal{L} : \Omega_0 \to \mathbb{R}^{n+1} : (s, t) \mapsto \Gamma(s) + \sum_{i=1}^{n} \Theta_i(s) N_i(s), \tag{1.1}$$

where the functions $\Theta_i : I \to \mathbb{R}$, $i \in \{1, \ldots, n\}$ satisfy

$$\sum_{i=1}^{n} \Theta_i^2(s) = 1 \quad \text{for all } s \in I\,, \tag{1.2}$$

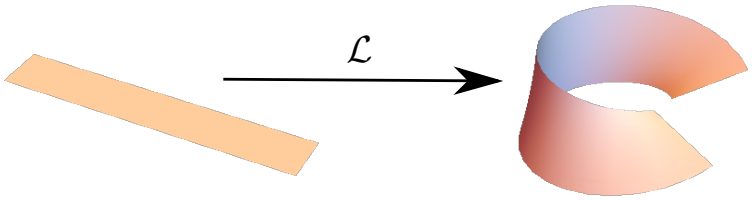

Figure 1.1: Example of a quantum ribbon in three dimensions along with the mapping $\mathcal{L}$ responsible for the creation of the curved strip.

and $\Theta_i \in C^{0,1}(I)$ for all $i \in \{1, \dots, n\}$. We introduce the notation of $\Theta := (\Theta_1, \dots, \Theta_n)$ and call the vector Θ *the twisting function*. Then the image Ω of Ω_0 via the mapping $\mathcal{L}$, $\Omega := \mathcal{L}(\Omega_0)$, is called *the curved strip*. If the twisting function is a constant vector, then we say that the strip is *purely bent*, on the other hand, when the scalar product of the curvature and the twisting function $k \cdot \Theta$ vanishes and the deformation is caused solely by twisting, the resulting strip is called *purely twisted*. In this sense, the product $k \cdot \Theta$ acts as the geodesic curvature in three dimensions.

Example 1.1. Let us briefly examine the situation in three dimensions first. Here, the condition in (1.2) imposed on Θ characterize the first row/column of an arbitrary rotation matrix $\mathcal{R}$. Namely,

$$\mathcal{R} = \begin{pmatrix} \cos\theta & -\sin\theta \\ \sin\theta & \cos\theta \end{pmatrix}, \quad \Theta := (\cos\theta, -\sin\theta) .$$

Therefore, the mapping can be rewritten in more explicit form as

$$\mathcal{L} : \Omega_0 \to \mathbb{R}^3 : (s,t) \mapsto \Gamma(s) + t\,[N_1(s)\cos\theta(s) - N_2(s)\sin\theta(s)]\,, \tag{1.3}$$

for some function $\theta : I \to \mathbb{R}$, $\theta \in W^{1,\infty}_{loc}(I)$, $\dot\theta \in L^\infty(I)$. Let us abuse the terminology here and call it *the twisting function* as well, for our convenience. An example of a quantum ribbon in three dimensions can be found in Fig. 1.1.

Returning to the more general setting, further conditions must be imposed on the mapping $\mathcal{L}$ in order to identify the curved strip Ω with a Riemannian manifold. Namely, these conditions are

1. $\kappa := \sqrt{k_1^2 + \dots + k_n^2} \in L^\infty(I)$ and $a\|k \cdot \Theta\|_\infty < 1$,
2. Ω does not overlap itself.

Specifically, the second condition means that the mapping $\mathcal{L}$ is injective. Recall that thanks to the condition (1.2) imposed on Θ, κ is also the upper bound to $k \cdot \Theta$ as $|k \cdot \Theta| \le |k||\Theta| = \kappa$.

Focusing on the properties of a ribbon defined by (1.1) as a Riemannian manifold, the metric g, given by $g_{ij} := \partial_i \mathcal{L} \cdot \partial_j \mathcal{L}$, reads

$$(g_{ij}) = \begin{pmatrix} f^2 & 0 \\ 0 & 1 \end{pmatrix}, \tag{1.4}$$

where

$$f(s,t)^2 = (1 - t\, k(s) \cdot \Theta(s))^2 + t^2 \sum_{i=1}^{n} \Theta_i'(s)^2$$

with Θ_i being the components of the twisting function Θ and k_i being the parallel curvatures of the relatively parallel adapted frame used in the definition of the strip. Additionally, the resulting Laplace–Beltrami operator acting on $L^2(\Omega_0, f\,\mathrm{d}s\,\mathrm{d}t)$ in local coordinates is given by

$$-\Delta = -\frac{1}{f}\,\partial_1 \frac{1}{f}\,\partial_1 - \frac{1}{f}\,\partial_2\, f\,\partial_2\,. \tag{1.5}$$

By employing the unitary transform $U_f : L^2(\Omega_0, f\,\mathrm{d}s\,\mathrm{d}t) \to L^2(\Omega_0, \mathrm{d}s\,\mathrm{d}t)$, $U_f(-\Delta) := f^{1/2}(-\Delta)f^{-1/2}$, and rearranging the expression, the transformed operator reads

$$-\partial_1 \frac{1}{f^2}\partial_1 - \partial_2^2 + V,$$

where the potential V is given by

$$V = -\frac{5}{4}\frac{f_{,1}^2}{f^4} + \frac{1}{2}\frac{f_{,11}}{f^3} - \frac{1}{4}\frac{f_{,2}^2}{f^2} + \frac{1}{2}\frac{f_{,22}}{f}\,.$$

Here onwards, the notation with commas is used to indicate a partial derivative, *i.e.* $f_{,1}(s,t) := \frac{\partial f}{\partial s}(s,t)$. This transformed operator is used later in Chapters 2 and 3, as it is sometimes more convenient to work without the metric function f and with the potential V instead. By a *nanoribbon*, we understand an arbitrarily curved ribbon on which we define the Laplace–Beltrami operator.

Lastly, let us introduce some additional notations. Firstly, we shorten the notation for vectors k and Θ in the following way

$$\begin{aligned} \|k\| &\equiv \||k|\|\,, \\ \|\Theta'\| &\equiv \||\Theta'|\|\,. \end{aligned}$$

Also, by $W^{1,2}(\Omega_0, g)$, we understand

$$W^{1,2}(\Omega_0, g) = \left\{ \psi \in L^2(\Omega_0, f(s,t)\,\mathrm{d}s\ \mathrm{d}t) \,\middle|\, \int_{\Omega_0} \psi_{,j}(s,t) g^{jk} \psi_{,k}(s,t) f(s,t)\,\mathrm{d}s\ \mathrm{d}t \right\}$$

and $\|.\|$ stands for $\|.\|_{L^2(\Omega_0,g)}$.

And finally, we use the same notations for functions w, $w \otimes 1$ and $1 \otimes w$.

Chapter 2

Spectral properties

In this chapter, spectral results for several different cases of quantum nanoribbons are presented. The organisation is as follows – the quantum Hamiltonian is introduced in the first section, followed by the spectral properties of asymptotically flat strips, purely bent strips, and, finally, by Hardy inequalities in twisted strips. The results in this chapter are usually generalizations of results found in [28, 32, 13, 33].

As one of the main motivations for the study of quantum nanoribbons lies with the investigation of the transport properties in nano-structures, which are usually considered as infinite for 'practical' applications, we solely interest ourselves with infinite ribbons throughout this chapter. Beyond this assumption that the considered ribbons are supported on infinite curves, *i.e.* $\Gamma : \mathbb{R} \to \mathbb{R}^{n+1}$, we impose some further basic restrictions on all our strips, namely:

$$\langle\star\rangle \qquad \begin{cases} \Omega \text{ is not self–intersecting,} \\ \kappa \in L^\infty(\mathbb{R}) \text{ with } a\|k \cdot \Theta\|_\infty < 1\,, \\ \Theta' \in L^\infty(\mathbb{R})\,. \end{cases}$$

2.1 Proper introduction of the quantum Hamiltonian

Let $\Omega_0 := \mathbb{R} \times (-a, a)$ be a flat strip, which is then bent and/or twisted by mapping the $\mathcal{L}$ into an arbitrary strip Ω as we observed in Chapter 1 according to our standing assumptions $\langle\star\rangle$. We introduce the quantum Hamiltonian corresponding to the Laplace–Beltrami operator (1.5) on Ω by the means of the following procedure.

Firstly, we identify Ω with Ω_0 through unitary transformation by using curvilinear coordinates, thus $\Omega \cong (\Omega_0, g)$, where

$$(g_{ij}) = \begin{pmatrix} f^2 & 0 \\ 0 & 1 \end{pmatrix}$$

is the metric induced by $\mathcal{L}$. Its inverse and determinant are denoted by (g^{ij}) and g respectively. Recall that the function f is defined as

$$f(s,t) = \sqrt{(1 - t\,k(s) \cdot \Theta(s))^2 + t^2 \|\Theta'(s)\|^2}\,,$$

and the Hilbert space is then given by $\mathscr{H} = L^2(\Omega_0, f\,\mathrm{d}s\,\mathrm{d}t)$.

Next, we consider the quadratic form $\dot{h}$ prescribed as

$$\begin{cases} \dot{h}[\psi] := \displaystyle\int_{\Omega_0} \frac{|\psi_{,1}|^2}{f} + \int_{\Omega_0} |\psi_{,2}|^2 f\,, \\ \mathrm{Dom}\left(\dot{h}\right) := C_0^\infty(\Omega_0)\,. \end{cases}$$

It is easy to see that $\dot{h}$ is densely defined, symmetric and bounded from below. It, however, is not closed. Therefore, we define its closure h:

$$\begin{cases} h := \overline{\dot{h}} \\ \mathrm{Dom}\,(h) := \overline{C_0^\infty(\Omega_0)}^{|||.|||} \end{cases}$$

where the norm $|||.|||$ is given by

$$\begin{aligned} |||\psi|||^2 &:= \int_{\Omega_0} \frac{|\psi_{,1}|^2}{f} + \int_{\Omega_0} |\psi_{,2}|^2 f + \int_{\Omega_0} |\psi|^2 f \\ &= \dot{h}[\psi] + \|\psi\|^2_{\mathscr{H}}\,. \end{aligned}$$

To prove that the norm $|||.|||$ is equivalent with $\|.\|_{W^{1,2}(\Omega_0)}$, one must show that there exist constants c_-, C_+ such that the metric function f can be bounded as

$$0 < c_- \leq f(s,t) \leq C_+ < \infty\,.$$

The lower bound can be found using the Cauchy–Schwarz inequality

$$f^2 \geq (1 - |t||k \cdot \Theta|)^2 \geq (1 - a|k|)^2 \geq (1 - a\|k\|_\infty)^2$$

Similarly, the upper bound in $n+1$ dimensions is given by

$$f^2 \leq (1 + |t||k \cdot \Theta|)^2 + |t|^2\|\Theta'\|^2 \leq (1 + a\|k\|_\infty)^2 + a^2 n\|\Theta'\|^2 \leq 2^2 + a^2 n\|\Theta'\|^2 .$$

Thus, the norms are equivalent when the following holds:

$$a\|k \cdot \Theta\|_\infty < 1 \quad \text{and} \quad \Theta' \in L^\infty(\mathbb{R}) .$$

Please note that these are the conditions already imposed on the strip in $\langle\star\rangle$.

Therefore, we conclude that the operator H associated by the representation theorem (see *e.g.* [38, Thm. VI.2.6]) with the quadratic form h is well defined as

$$\begin{aligned} \mathrm{Dom}(H) &:= \{\psi \in \mathrm{Dom}(h) \,|\, \exists \eta \in \mathscr{H},\, \forall \phi \in \mathrm{Dom}(h),\, h(\phi, \psi) = (\phi, \eta)\} , \\ H\psi &:= \eta . \end{aligned}$$

2.2 Asymptotically flat strips

In this section, we tackle the spectral problem of asymptotically flat infinite strips. Localization of the essential spectra of those strips is provided, with the result being the positive real numbers bigger or equal to the first eigenvalue in the transverse direction.

Asymptotically flat strips need to fulfil the following conditions:

$$f \to 1 \quad \text{as} \quad |s| \to \infty ,$$

where by $f \to 1$ we mean that f tends to one uniformly. The necessary and sufficient conditions for that are

$$\begin{aligned} k \cdot \Theta &\to 0 \quad \text{as} \quad |s| \to \infty , \\ \Theta' &\to 0 \quad \text{as} \quad |s| \to \infty , \end{aligned} \tag{2.1}$$

where the latter means

$$|\Theta'| \to 0 \quad \text{as} \quad |s| \to \infty .$$

Firstly, we establish a lower bound on the essential spectrum $\sigma_{\mathrm{ess}}(H)$ in the following Theorem.

Theorem 2.1. *Assume $\langle\star\rangle$ along with the strip Ω being asymptotically flat,* i.e. *that the conditions* (2.1) *hold.*

Then

$$\inf \sigma_{\mathrm{ess}}(H) \geq E_1,$$

where $E_1 = \left(\frac{\pi}{2a}\right)^2$ is the first eigenvalue of the Dirichlet Laplacian in the interval $(-a, a)$.

Proof. Let us fix some arbitrary $s_0 > 0$. Then we can divide Ω into an interior and exterior part with respect to s_0 as follows

$$\begin{aligned}\Omega_0^{\mathrm{int}} &:= (-s_0, s_0) \times (-a, a)\\ \Omega_0^{\mathrm{ext}} &:= \Omega_0 \setminus \overline{\Omega_0^{\mathrm{int}}}\,.\end{aligned}$$

Imposing the Neumann boundary condition on the boundary of Ω_0^{int} and Ω_0^{ext}, the original Hamiltonian H is decoupled into an interior and exterior part

$$H^{\mathrm{N}} = H^{\mathrm{N}}_{\mathrm{int}} \oplus H^{\mathrm{N}}_{\mathrm{ext}},$$

where the $H^{\mathrm{N}}_{\mathrm{int}}$ and $H^{\mathrm{N}}_{\mathrm{ext}}$ are associated with the quadratic forms

$$\begin{aligned}Q^{\mathrm{N}} &:= Q^{\mathrm{N}}_{\mathrm{int}} \oplus Q^{\mathrm{N}}_{\mathrm{ext}},\\ \mathrm{Dom}(Q^{\mathrm{N}}) &:= \mathrm{Dom}(Q^{\mathrm{N}}_{\mathrm{int}}) \oplus \mathrm{Dom}(Q^{\mathrm{N}}_{\mathrm{ext}}),\\ Q^{\mathrm{N}}_{\omega}(\psi, \phi) &:= (\psi_i, g^{ij}\phi_j)_{\mathscr{H}},\\ \mathrm{Dom}(Q^{\mathrm{N}}_{\omega}) &:= \{\psi \in W^{1,2}(\Omega_0^{\omega}, g) \,|\, \psi(\,.\,, \pm a) = 0\}\end{aligned}$$

acting on

$$\mathscr{H}_{\omega} := L^2(\Omega_0^{\omega}, f\,\mathrm{d}s\,\mathrm{d}t),$$

where $\omega \in \{\mathrm{int}, \mathrm{ext}\}$ and the condition $\psi(\,.\,, \pm a) = 0$ is understood in the trace sense. It follows that

$$H \geq H^{\mathrm{N}},$$

from which the minimax principle gives us the following inequality

$$\inf \sigma_{\mathrm{ess}}(H) \geq \inf \sigma_{\mathrm{ess}}(H^{\mathrm{N}})\,.$$

The spectrum of $H^{\mathrm{N}}_{\mathrm{int}}$ is purely discrete, therefore it is sufficient to find the lower bound on the operator $H^{\mathrm{N}}_{\mathrm{ext}}$. The following estimates are valid for all $\psi \in \mathrm{Dom}(Q^{\mathrm{N}}_{\mathrm{ext}})$:

$$\begin{aligned}Q^{\mathrm{N}}_{\mathrm{ext}}[\psi] \geq \|\psi_{,2}\|^2_{\mathscr{H}_{\mathrm{ext}}} &\geq (\inf_{\Omega_0^{\mathrm{ext}}} f)\|\psi_{,2}\|^2_{L^2(\Omega_0^{\mathrm{ext}})} \geq (\inf_{\Omega_0^{\mathrm{ext}}} f)E_1\|\psi\|^2_{L^2(\Omega_0^{\mathrm{ext}})}\\ &\geq (\inf_{\Omega_0^{\mathrm{ext}}} f)(\sup_{\Omega_0^{\mathrm{ext}}} f)^{-1}E_1\|\psi\|^2_{\mathscr{H}_{\mathrm{ext}}}\,.\end{aligned}$$

After dividing by the norm of ψ, the result reads

$$\frac{Q^{\mathrm{N}}_{\mathrm{ext}}[\psi]}{\|\psi\|^2_{\mathscr{H}_{\mathrm{ext}}}} \geq E_1 \frac{\inf_{\Omega_0^{\mathrm{ext}}} f}{\sup_{\Omega_0^{\mathrm{ext}}} f}\,.$$

Performing the limit $s_0 \to \infty$, the asymptotic flatness of the strip ensures that

$$\inf \sigma_{\mathrm{ess}}(H) \geq \inf \sigma_{\mathrm{ess}}(H^{\mathrm{N}}_{\mathrm{ext}}) \geq \left(\frac{\pi}{2a}\right)^2 (1 + \mathcal{O}(1))\,,$$

and therefore, the right–hand side tends to E_1 while the left–hand side is independent on s_0. □

Having the lower bound on the essential spectrum, we can now localize it further by the subsequent theorem.

Theorem 2.2. *Suppose* $\langle\star\rangle$. *If the strip is in addition asymptotically flat,* i.e. *conditions* (2.1) *holds, then*

$$\sigma_{\mathrm{ess}}(H) = \left[\left(\frac{\pi}{2a}\right)^2, +\infty\right).$$

Proof. From Theorem 2.1, it follows that $\inf \sigma_{\mathrm{ess}}(H) \geq \left(\frac{\pi}{2a}\right)^2 = E_1$ and so it only remains to prove that all $\eta \in [E_1, +\infty)$ are in the essential spectrum of our operator. The proof itself is based on the Weyl criterion adapted to the quadratic forms, as can be found in [29] or [28]. It states that to prove η is in the essential spectrum of the operator H, it is enough to find a sequence $\{\psi_n\}_{n=1}^{\infty} \subset \mathrm{Dom}(h)$ such that

1. $\forall n \in \mathbb{N},\ \|\psi_n\| = 1\,,$
2. $\|(H - \eta)\,\psi_n\|_{[\mathrm{Dom}(h)]^*} \overset{n\to\infty}{\longrightarrow} 0\,,$

where $[\mathrm{Dom}(h)]^*$ denotes the dual space of $\mathrm{Dom}(h)$. Recall that the mapping $H + 1 : \mathrm{Dom}(h) \to [\mathrm{Dom}(h)]^*$ is an isomorphism and that the norm $\|.\|_{[\mathrm{Dom}(h)]^*}$ is defined as

$$\|\psi\|_{-1} := \|\psi\|_{[\mathrm{Dom}(h)]^*} = \sup_{\phi \in \mathrm{Dom}(h), \phi \neq 0} \frac{|(\phi, \psi)|}{\|\phi\|_1}$$

with

$$\|\phi\|_1 \equiv |||\psi||| \equiv \|\psi\|_{\mathrm{Dom}(h)} := \sqrt{h[\phi] + \|\phi\|^2}\,.$$

The advantage of this characterization is that the sequence $\{\psi_n\}_{n=1}^{\infty}$ has to be in the domain of the quadratic form h only, in contrast to the normal Weyl criterion, where it must be from $\mathrm{Dom}(H)$.

We choose η in a special form $\eta = \lambda^2 + \left(\frac{\pi}{2a}\right)^2 = \lambda^2 + E_1$, $\forall \lambda \in \mathbb{R}$, which encompasses precisely the whole interval $[E_1, +\infty)$. Let us start with the sequence $\{\hat{\psi}_n\}_{n=1}^{\infty}$, where ψ_n is given as

$$\hat{\psi}_n(s,t) = \varphi_n(s)\,\chi_1(t)\,\mathrm{e}^{i\lambda s}$$

with χ_1 being the first eigenfunction in the transverse direction,

$$\chi_1(t) = \sqrt{\frac{1}{a}}\sin\sqrt{E_1}t\,, \tag{2.2}$$

and φ_n being

$$\varphi_n(s) = \varphi\left(\frac{s}{n} - n\right),$$

where φ is any smooth function such that $\varphi \in C^\infty$, $\varphi \not\equiv 0$, $\operatorname{supp}\varphi \subset (-1,1)$. This ensures that $\operatorname{supp}\varphi_n \subset (n^2 - n, n^2 + n)$ and thus φ_n is for large n localised at infinity. Also note that $\chi_1(t)\,\mathrm{e}^{i\lambda s}$ formally solves our spectral problem for a straight strip but, alas, does not belong to the domain of h.

Clearly, $\hat{\psi}_n \in \mathrm{Dom}\,(h)$ as for all $n \in \mathbb{N}$, $\hat{\psi}_n(s, \pm a) = 0$ thanks to χ_1 and $\hat{\psi}_n \in W^{1,2}(\Omega_0, g)$. However, $\hat{\psi}_n$ is not normalised, so we define the normalised sequence

$$\psi_n := \frac{\hat{\psi}_n}{\|\hat{\psi}_n\|}.$$

Let us recall that $\|.\| \equiv \|.\|_{L^2(\Omega_0,g)}$. Now the sequence $\{\psi_n\}$ satisfies the first condition of the modified Weyl criterion and it is necessary to check only the second one.

As our metric (g_{ij}) is in the diagonal form (see (1.4)), the Hamiltonian can be decomposed as

$$H = H_1 + H_2,$$

where H_1, H_2 are corresponding to the term g^{11} and g^{22} respectively, and the whole decomposition is understood in the sense of forms. This decomposition leads to a trivial bound of

$$\|(H - \eta)\,\psi_n\|_{-1} \leq \|\left(H_1 - \lambda^2\right)\psi_n\|_{-1} + \|(H_2 - E_1)\,\psi_n\|_{-1}\,,$$

for which we show that the two norms on the right–hand side tend to zero separately as $n \to \infty$.

Writing out the norm $\|.\|_{-1}$, we can estimate the second term as

$$\|(H_2 - E_1)\,\psi_n\|_{-1} \leq \frac{\sqrt{E_1}}{c_-}\,\|\phi\|_{L^2(\Omega_0,g)}\,\|f_{,2}\|_{\infty,n}\,\|\psi_n\|_{L^2(\Omega_0,g)},$$

where $\|f_{,2}\|_{\infty,n}$ stands for

$$\|w\|_{\infty,n} := \sup\{|w(s,t)| \,|\, (s,t) \in \operatorname{supp}\varphi_n \times (-a,a)\}\,.$$

The convergence to zero is obtained due to the derivative of the metric function f, since we assume an asymptotically flat strip, for which f tends to 1 uniformly in both infinities and therefore, its derivative with respect to the transverse variable tend to 0 in $\operatorname{supp}\varphi_n \times (-a,a)$ for $n \to \infty$.

As for the first term, we get the following estimate

$$\begin{aligned}\left(\phi, \left(H_1 - \lambda^2\right)\psi_n\right) \leq \lambda^2 \left(\phi, (1-f)\,\psi_n\right)_{L^2(\Omega_0)} \\ + \left(\phi_{,1}, \left(\frac{1}{f} - 1\right)(\varphi_n + i\lambda\varphi_n)\,\chi_1 \mathrm{e}^{i\lambda s}\right)_{L^2(\Omega_0)} \\ - \left(\phi, (\ddot{\varphi} + 2i\lambda\dot{\varphi})\,\chi_1 \mathrm{e}^{i\lambda s}\right)_{L^2(\Omega_0)}.\end{aligned}$$

Since all the terms

$$\|1-f\|_{\infty,n}\,, \quad \|\frac{1}{f} - 1\|_{\infty,n}\,, \quad \frac{\|\dot{\varphi}_n\|_{L^2(\mathbb{R})}}{\|\varphi_n\|_{L^2(\mathbb{R})}}\,, \quad \frac{\|\ddot{\varphi}_n\|_{L^2(\mathbb{R})}}{\|\varphi_n\|_{L^2(\mathbb{R})}}$$

tend to 0 as $n \to \infty$ thanks to either the assumptions or definition of φ, the first term has the zero as a limit as well. □

2.3 Purely bent strips

In this section, spectral properties of purely bent ribbons are discussed. These strips are constructed in such a way that the twisting function is constant, reducing the metric function in this case to

$$f_\kappa(s,t) = 1 - t\,k(s)\cdot\Theta(s)\,.$$

We will show that due to the bending, the discrete spectrum of the Laplace–Beltrami operator on such strips is not empty, resulting in the manifestation of bound states.

Theorem 2.3. *Suppose $\langle\star\rangle$ along with $\Theta = const$.*

If $k\cdot\Theta \not\equiv 0$, then

$$\inf\sigma(H) < E_1\,.$$

Consequently, if the strip is not flat but the scalar product of curvature and twisting function vanishes at infinity, then H has at least one eigenvalue of finite multiplicity below its essential spectrum $[E_1,\infty)$, i.e. $\sigma_{disc}(H) \neq \emptyset$.

Proof. The proof is based on the variational strategy of finding a trial function $\psi \in \mathrm{Dom}(H)$ which satisfies

$$h_1[\psi] := h[\psi] - E_1\|\psi\|^2 < 0\,. \tag{2.3}$$

We wish to achieve that by modifying the first transversal eigenfunction of the straight strip χ_1, defined in (2.2). Firstly, consider the following trial function

$$\psi_n(s,t) := \varphi(s;n)\chi_1(t)\,, \tag{2.4}$$

where $\varphi : \mathbb{R}\times(0,\infty) \to [0,1]$ is a suitable mollifier of identity, *i.e.* it satisfies the following conditions

1. $\forall n \in \mathbb{N}$, $\varphi(.;n) \in W^{1,2}(\mathbb{R})$,
2. $\varphi(s;n) \overset{n\to\infty}{\longrightarrow} 1$ for almost every $s \in \mathbb{R}$,
3. $\|\varphi_{,1}(.;n)\|_{L^2(\mathbb{R})} \overset{n\to\infty}{\longrightarrow} 0$.

Example of such function could be

$$\varphi_c(s;n) := \begin{cases} 1 & |s| \in (0,n) \\ \frac{cn-|s|}{(c-1)n} & |s| \in [n,cn) \\ 0 & |s| \geq cn \end{cases}$$

defined for all $c > 1$. Let us use $\varphi_2(s;n)$ and denote it by $\varphi_n(s)$.

When we calculate $h_1[\psi_n]$ for ψ_n defined as in (2.4), the final expression reads

$$h_1[\psi_n] = \left(\varphi_{n,1}, \left\langle \frac{1}{f_\kappa} \right\rangle \varphi_{n,1}\right)_{L^2(\mathbb{R}^2)}\,,$$

where $\langle . \rangle$ is given by

$$\langle u \rangle := \int_{-a}^{a} u\,\chi_1^2(t)\,\mathrm{d}\,t\,, \quad u \in L^\infty(\Omega_0)\,.$$

Hence, due to the third condition on the function φ,

$$h_1[\psi_n] \overset{n\to\infty}{\longrightarrow} 0\,. \tag{2.5}$$

To get the desired result (2.3), we modify the trial function ψ_n in the following way

$$\psi_{n,\varepsilon}(s,t) := \psi_n(s,t) - \varepsilon\frac{t}{a}\phi(s)\,\chi_1(t)\,,$$

where $\varepsilon \in \mathbb{R}$ and $\phi \in W^{1,2}(\mathbb{R})$ is a real, non–negative, non–zero function with compact support contained in a bounded interval in $\mathbb{R}$ where $k\cdot\Theta \not\equiv 0$, and

which does not change sign. The family of functions $\{\psi_{n,\varepsilon}\}$ are, indeed, a subset of $\mathrm{Dom}(h_1)$ and, by explicit calculation, we find that

$$h_1[\psi_{n,\varepsilon}] = h_1[\psi_n] - 2\varepsilon h_1\left(\frac{t}{a}\,\phi\,\chi_1, \psi_n\right) + \varepsilon^2 h_1\left[-\frac{t}{a}\,\phi\,\chi_1\right]. \tag{2.6}$$

The first term on the right–hand side of (2.6) tends to zero as $n \to \infty$ by (2.5), while the last term does not depend on n. The central term yields

$$h_1\left(\frac{t}{a}\,\phi\,\chi_1, \psi_n\right) = \left(\phi', \left\langle -\frac{t}{a}\frac{1}{f}\right\rangle \varphi_{n,1}\right)_{L^2(\mathbb{R})} + \frac{1}{2a}\left(\phi, k\cdot\Theta\ \varphi_n\right)_{L^2(\mathbb{R})},$$

with the first term on the right–hand side tending to zero as $n \to \infty$ due to the properties of the function φ. Overall, we obtain

$$h_1[\psi_{n,\varepsilon}] \overset{n\to\infty}{\longrightarrow} \varepsilon^2 h_1\left[-\frac{t}{a}\phi\chi_1\right] - \frac{\varepsilon}{a}\left(\phi, k\cdot\Theta\right)_{L^2(\mathbb{R})}.$$

Since the second term is non–zero by the construction of ϕ, by choosing ε sufficiently small and of an appropriate sign we can make the sum on the right–hand side negative. Thus, for sufficiently large n, we are able to make

$$h_1[\psi_{n,\varepsilon}] < 0$$

as requested. □

2.4 Hardy inequalities on twisted strips

The last section of this chapter is devoted to presenting several Hardy inequalities on (purely) twisted strips. For obtaining such a purely twisted strip, the sufficient condition is that the product $k\cdot\Theta \equiv 0$. Hence, the metric is given as

$$g_\Theta = \begin{pmatrix} f_\Theta^2 & 0 \\ 0 & 1 \end{pmatrix}, \quad \text{with} \quad f_\Theta(s,t) := \sqrt{1 + (t\,\Theta'(s))^2}\,. \tag{2.7}$$

For these strips, we can derive the following Hardy inequality, which bounds the spectrum from below and therefore forbids the manifestation of bound states.

Theorem 2.4. *Suppose $\langle\star\rangle$ as well as that the metric on the strip Ω fulfils (2.7). Further assume that Θ' is not identically zero and that $a\|\Theta'\|_\infty < \sqrt{2}$.*

Then, for all $\psi \in W_0^{1,2}(\mathbb{R}\times(-a,a))$ and any s_0 such that $\Theta'(s_0) \neq 0$, we have

$$h_\Theta[\psi] - E_1\|\psi\|^2_{\mathscr{H}_\Theta} \geq c\|\rho^{-1}\psi\|^2_{\mathscr{H}_\Theta} \quad \textit{with} \quad \rho(s,t) := \sqrt{1+(s-s_0)^2}, \tag{2.8}$$

where c is a positive constant depending on s_0, a, and Θ'.

Since the proof of this theorem is rather long and technical, we prepare two auxiliary lemmas first.

Let us introduce function $\lambda : \mathbb{R} \to \mathbb{R}$ by

$$\lambda(s) := \inf_{\varphi \in C_0^\infty((-a,a)), \varphi \neq 0} \frac{\int_{-a}^{a} |\dot{\varphi}(t)|^2 f_\Theta(s,t)\,\mathrm{d}t}{\int_{-a}^{a} |\varphi(t)|^2 f_\Theta(s,t)\,\mathrm{d}t} - E_1\,. \tag{2.9}$$

We can then prove the following.

Lemma 2.5. *Under the assumptions of Theorem 2.4, λ is a non–negative function which is not identically zero.*

Proof. For any fixed $s \in \mathbb{R}$, employing the change of the test function $\phi := \sqrt{f_\Theta}\varphi$ and by integrating by parts, we obtain

$$\lambda(s) = \inf_{\phi \in C_0^\infty((-a,a)), \phi \neq 0} \frac{\int_{-a}^{a} \left(|\dot{\phi}(t)|^2 - E_1|\phi(t)|^2 + V(s,t)|\phi(t)|^2 \right) \mathrm{d}t}{\int_{-a}^{a} |\phi(t)|^2\,\mathrm{d}t},$$

where

$$V(s,t) := \frac{(\Theta(s)')^2 \left(2 - t^2(\Theta(s)')^2\right)}{4 f_\Theta(s,t)^4}.$$

Due to the assumptions of Theorem 2.4, the function V is non–negative and not identically zero. Combining this with the Poincaré inequality $\int_{-a}^{a} |\dot{\phi}|^2 \geq \int_{-a}^{a} |\phi|^2$, which is valid for all $\phi \in C_0^\infty((-a,a))$, we arrive at the claim of the lemma. □

Using the conclusion of Lemma 2.5 with the definition of λ (2.9), the following estimate is obtained

$$h_\Theta[\psi] - E_1 \|\psi\|^2_{\mathscr{H}_\Theta} \geq \|f_\Theta^{-1} \partial_1 \psi\|^2_{\mathscr{H}_\Theta} + \|\lambda^{1/2}\psi\|^2_{\mathscr{H}_\Theta}, \tag{2.10}$$

which is valid for all $\psi \in C_0^\infty(\mathbb{R} \times (-a,a))$. If we forget about the first term on the right–hand side of (2.10), the rest is already a Hardy inequality. However, as this form is not very convenient for applications, one can replace the Hardy weight λ in (2.10) with the positive function $c\rho^{-2}$ from Theorem 2.4 by exploiting the contribution of the first term as can be seen in the following Lemma by [33].

Lemma 2.6. *For any $\psi \in C_0^\infty(\mathbb{R} \times (-a,a))$,*

$$\left(1 + a^2 \|\Theta'\|^2_\infty\right)^{-1/2} \|\rho^{-1}\psi\|^2_{\mathscr{H}_\Theta} \leq 16 \left(1 + a^2 \|\Theta'\|^2_\infty\right)^{1/2} \|f_0^{-1}\partial_1\psi\|^2_{\mathscr{H}_\Theta} + \left(2 + \frac{64}{|I|^2}\right) \|\chi_I \psi\|^2_{\mathscr{H}_\Theta},$$

where I is any bounded subinterval of $\mathbb{R}$, χ_I is the characteristic function of the set $I \times (-a,a)$ and ρ is defined as in (2.8) with s_0 being the centre of the interval I.

Proof. The Lemma is a variation of the consecutive version of the one–dimensional Hardy inequality

$$\int_{\mathbb{R}} \frac{|u(x)|^2}{x^2}\,\mathrm{d}x \leq 4\int_{\mathbb{R}} |\dot{u}(x)|^2\,\mathrm{d}x, \tag{2.11}$$

which is valid for all $u \in W^{1,2}(\mathbb{R})$, for which $u(0) = 0$. Putting $b := \frac{|I|}{2}$, let us define the function $w : \mathbb{R} \to [0,1]$ by

$$w(s) := \begin{cases} 1 & \text{if } |s-s_0| \geq b\,, \\ \frac{|s-s_0|}{b} & \text{if } |s-s_0| < b\,. \end{cases}$$

We can write $\psi = w\psi + (1-w)\psi$ for any $\psi \in C_0^\infty(\mathbb{R}\times(-a,a))$. Using (2.11) for the function $s \mapsto (w\psi)(s,t)$, keeping the t fixed and integrating over $\mathbb{R}\times(-a,a)$, one obtains

$$\begin{aligned}\int \frac{|\psi|^2}{\rho^2} &\leq 2\int \frac{|w\psi|^2}{\rho^2-1} + 2\int \chi_I |(1-w)\psi|^2 \\ &\leq 16\int \left(|\partial_1 w|^2|\psi|^2 + |w|^2|\partial_1\psi|^2\right) + 2\int \chi_I|(1-w)\psi|^2 \\ &\leq 16\int |\partial_1\psi|^2 + \left(2+\frac{16}{b^2}\right)\int \chi_I|\psi|^2\,.\end{aligned}$$

Using the estimates for f_Θ

$$1 \leq f_\Theta^2 \leq 1 + a^2\|\Theta'\|_\infty^2$$

along with the definition of $\mathscr{H}_\Theta$, we arrive at the claim of the Lemma. □

Now we can return to the proof of Theorem 2.4.

Proof of Theorem 2.4. As it is sufficient, we consider only functions ψ from the dense subspace $C_0^\infty(\mathbb{R}\times(-a,a))$. Using the conclusion of Lemma 2.5, let I be any closed interval on which λ is positive. Using

$$\|\lambda^{1/2}\psi\|^2_{\mathscr{H}_\Theta} = \varepsilon\|\lambda^{1/2}\psi\|^2_{\mathscr{H}_\Theta} + (1-\varepsilon)\|\lambda^{1/2}\psi\|^2_{\mathscr{H}_\Theta}\,,$$

where $\varepsilon \in (0,1]$, neglecting the second term, and estimating the first one by an integral over $I\times(-a,a)$, we apply Lemma 2.6. The inequality (2.10) then reads

$$\begin{aligned} h_\Theta[\psi] - E_1\|\psi\|^2_{\mathscr{H}_\Theta} &\\ \geq \left[1 - 16\,\varepsilon\,(\min_I\lambda)\left(2+\frac{64}{|I|^2}\right)^{-1}\left(1+a^2\|\Theta'\|_\infty^2\right)^{1/2}\right]&\|f_\Theta^{-1}\partial_1\psi\|^2_{\mathscr{H}_\Theta} \\ + \varepsilon(\min_I\lambda)\left(2+\frac{64}{|I|^2}\right)^{-1}&\left(1+a^2\|\Theta'\|_\infty^2\right)^{-1/2}\|\rho^{-1}\psi\|^2_{\mathscr{H}_\Theta}\,. \end{aligned}$$

Choosing ε to be the minimum from 1 and the value for which the first term on the right–hand side of the last estimate vanishes, we obtain the result of Theorem 2.4 with

$$c \geq \min\left\{ \frac{\min_I \lambda}{(2+64/|I|^2)(1+a^2\|\Theta'\|_\infty^2)^{1/2}}, \frac{1}{16(1+a^2\|\Theta'\|_\infty^2)} \right\}.$$

□

Moreover, we can prove a certain stability of the Hardy inequality against slight curving of the strip. This is due to the presence of twisting, which prevents the manifestation of bound states despite the strip being mildly bent.

Theorem 2.7. *Assume $\langle\star\rangle$ as well as that $\Theta' \not\equiv 0$ and $a\|\Theta'\|_\infty < \sqrt{2}$. Assume also that for all $s \in \mathbb{R}$*

$$|k \cdot \Theta| \leq \varepsilon(s) := \frac{\varepsilon_0}{1+s^2} \quad \text{for some} \quad \varepsilon_0 \in [0, a^{-1}).$$

Then there exists a positive constant C such that $\varepsilon_0 \leq C$ implies

$$H \geq E_1,$$

which we understand in the form sense and where C depends on a and on the constants c and s_0 from Theorem 2.4.

Proof. The proof is founded on a comparison and explicit computation of $h[\psi] - E_1\|\psi\|$ and $h_\Theta[\psi] - E_1\|\psi\|_{\mathscr{H}_\Theta}$, with the usage of Theorem 2.4. Let $\psi \in C_0^\infty(\Omega_0)$. Then for every $s \in \mathbb{R}$, we can estimate f/f_Θ as

$$f_-(s) := \sqrt{1 - \frac{2a\varepsilon(s) + a^2\varepsilon^2(s)}{1+a^2\|\Theta'\|_\infty^2}} \leq \frac{f(s,t)}{f_\Theta(s,t)} \leq 1 + a\varepsilon(s) =: f_+(s).$$

The lower bound is well defined and positive, with both bounds behaving like $1 + \mathcal{O}(\varepsilon(s))$ when $\varepsilon_0 \to 0$. We can thus state the following

$$\begin{aligned} h[\psi] - E_1\|\psi\|^2 \geq \int_{\Omega_0} f_+^{-1} f_\Theta^{-1} |\partial_1\psi|^2 \\ + \int_{\Omega_0} \left(|\partial_2\psi(s,t)|^2 - E_1|\psi(s,t)|^2 \right) f_-(s) f_\Theta(s,t) \, \mathrm{d}s \, \mathrm{d}t \\ - E_1 \int_{\Omega_0} (f_+ - f_-) f_\Theta |\psi|^2 . \end{aligned}$$

Further estimate, using the proof of the previous theorem, reads

$$\begin{aligned} h[\psi] - E_1\|\psi\|^2 \geq \min\{f_+^{-1}(0), f_-(0)\} \left(h_\Theta[\psi] - E_1\|\psi\|_{\mathscr{H}_\Theta}^2 \right) \\ - E_1 \int_{\Omega_0} (f_+ - f_-) f_\Theta |\psi|^2 . \end{aligned}$$

Using the result of Theorem, 2.4, we obtain an even stronger Hardy–type inequality

$$h[\psi] - E_1\|\psi\|^2 \geq \|\omega^{1/2}\psi\|^2_{\mathscr{H}_\Theta}\,,$$

where

$$\omega(s,t) := \frac{c\min\{f_+^{-1}(0), f_-(0)\}}{1+(s-s_0)^2} - E_1[f_+(s) - f_-(s)]$$

is positive for all sufficiently small ε_0. □

Combining this theorem with the localization of essential spectra for asymptotically flat strip 2.2, one immediately gets the subsequent corollary.

Corollary 2.8. *Assume that Θ' tends to zero as $|s| \to \infty$ as well as the premises of Theorem 2.7. Then*

$$\sigma(H) = [E_1, \infty)\,.$$

Proof. As Theorem 2.7 provides that there is no spectrum below E_1, we use the same method used in the proof of Theorem 2.2 to show that all $\eta \in [E_1, \infty)$ are in the spectrum $\sigma(H)$. Due to the upper bound $\varepsilon(s) = \frac{\varepsilon_0}{1+s^2}$ of $|k\cdot\Theta|$, $\|f_{,2}\|_{\infty,n}$, $\|1-f\|_{\infty,n}$ and $\|\frac{1}{f}-1\|_{\infty,n}$ all tend to zero as $n\to\infty$. Therefore, the whole spectrum coincides with the interval $[E_1,\infty)$. □

Chapter 3

Möbius strip

One particular example of a closed ribbon in $\mathbb{R}^3$ is the Möbius strip, which unorientability along with its similarity to either a cylinder or an annulus (Fig. 3.1) makes its analysis desirable. Throughout this chapter, three different models for the Möbius strip are considered – the fake, not–so–fake and full model. The first two are analytically solvable as can be seen in first two sections. However, as the last one resisted our attempts on finding analytical solutions, the second half of this chapter is devoted to numerical simulations of both the analytically solvable models and the full one. Comparisons of both the numerical approximations with the analytical solution for the not–so–fake model along with the behaviour of the full model in the narrow width limit are presented here. In order to justify the numerical solutions of the full model, we present a rigorous proof that, at least for narrow ribbons, the full model can be very well approximated by the not–so–fake one in the last section.

For the purpose of this thesis, we consider a circular Möbius strip with constant twisting defined as follows. Let the base circle be described as

$$\Gamma : (0, 2\pi) \to \mathbb{R}^3 : s \mapsto \left(R\cos\frac{s}{R}, R\sin\frac{s}{R}, 0 \right),$$

for some fixed $R > 0$. In this case, there is no advantage of choosing the relatively parallel adapted frame over the Frenet frame, as the latter is correctly defined for this choice of the curve and in fact coincides with the relatively parallel one, if the initial conditions are chosen as the vectors of the Frenet frame. By easy calculations, one gets the following expressions for the

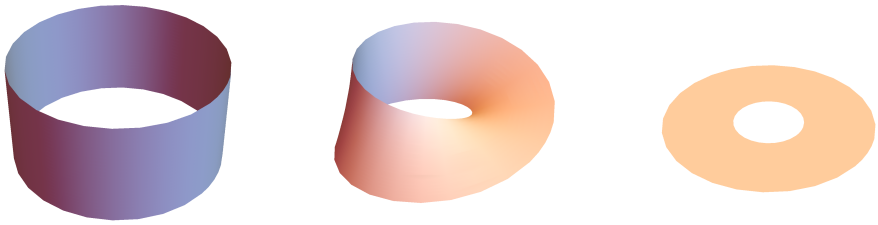

Figure 3.1: By different choice of the function θ in the construction of the ribbon (1.3), we can get different results. This particular example illustrates a ribbon along a circle with the $\theta = \frac{\pi}{2}, \frac{s}{2R}$ or 0 for the cylinder, Möbius strip and annulus respectively.

tangent, the principal normal, the binormal and the curvature respectively:

$$\begin{aligned} T(s) &= \left(-\sin\frac{s}{R}, \cos\frac{s}{R}, 0\right), \\ N(s) &= \left(-\cos\frac{s}{R}, -\sin\frac{s}{R}, 0\right), \\ B(s) &= (0,0,1), \\ \kappa(s) &= \frac{1}{R}. \end{aligned}$$

The time development then is given by

$$\begin{pmatrix} T \\ N \\ B \end{pmatrix}' = \begin{pmatrix} 0 & \kappa & 0 \\ -\kappa & 0 & 0 \\ 0 & 0 & 0 \end{pmatrix} \begin{pmatrix} T \\ N \\ B \end{pmatrix}.$$

We construct the Möbius strip by the mapping $\mathcal{L}$ (1.3) with a special choice on the "twisting" function θ and with 'identifying' the opposite ends of the strip. As we aim to obtain only a half of a twist for one rotation, the easiest way to do that is to set $\theta := \frac{s}{2R}$, which gives us constant twisting as well. Fixing the half width of the strip as some $a > 0$, the strip is then given by the following mapping

$$\mathcal{L}(s,t) := \Gamma(s) + t\left[N(s)\cos\frac{s}{2R} - B(s)\sin\frac{s}{2R}\right],$$

for $s \in (0, 2\pi R)$ and $t \in (-a, a)$. This mapping induces by the formula $g_{ij} := \partial_i\mathcal{L} \cdot \partial_j\mathcal{L}$ the metric

$$(g_{ij}) = \begin{pmatrix} f^2 & 0 \\ 0 & 1 \end{pmatrix},$$

where

$$f(s,t) = \sqrt{\left(1 - \frac{t}{R}\cos\frac{s}{2R}\right)^2 + \left(\frac{t}{2R}\right)^2}. \tag{3.1}$$

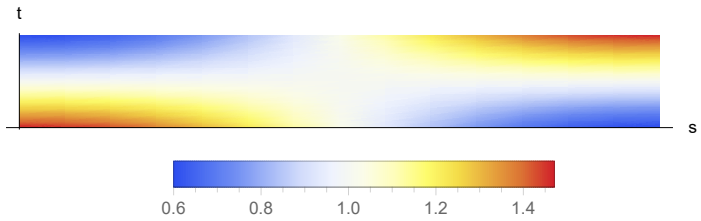

Figure 3.2: Density plot of the metric function f.

The density plot of the function f can be found on Fig. 3.2.

When computed, the Laplace–Beltrami operator (1.5) is not separable in this case. Therefore, some solvable approximations of the full Möbius strip as well as numerical solutions are presented instead. All subsequent calculations are for a Möbius strip of width $2a$ and length l, with the radius R being $R = \frac{l}{2\pi}$.

3.1 Fake Möbius strip

We will start the discussion of approximative models with the simplest setting – the fake (or flat) Möbius strip. In this case, the strip is perceived as a flat rectangle of the desired size with two of the opposing sides identified as indicated in Fig. 3.3. The sacrifice of the bending means that the Laplace–Beltrami operator is separable and thus the problem can be solved analytically as shown below.

Let $\Omega_0 := (0, l) \times (-a, a)$ and define a quadratic form h as

$$\begin{cases} h[\psi] := \int_{\Omega_0} |\nabla\psi|^2 \,, \\ \mathrm{Dom}(h) := \{\psi \in W^{1,2}(\Omega_0) \,|\, & \psi(s, \pm a) = 0 \quad \forall s \in (0, l), \\ & \psi(0, t) = \psi(l, -t) \quad \forall t \in (-a, a)\} \,. \end{cases}$$

Clearly, h is symmetric, bounded from below, closed and densely defined. By the representation theorem ([38, Thm. VI.2.6]), the operator H

$$\begin{aligned} \mathrm{Dom}(H) &:= \{\psi \in \mathrm{Dom}(h) \,|\, \exists \eta \in \mathscr{H}, \forall \phi \in \mathrm{Dom}(h),\, h(\phi, \psi) = (\phi, \eta)\} \,, \\ H\psi &:= \eta \,. \end{aligned}$$

associated with the form h is bounded from below and self–adjoint.

Figure 3.3: The fake Möbius strip - a rectangle with two of the opposite sides identified by the arrows.

However, let us consider the boundary value problem

$$\begin{cases} -\Delta\psi = \lambda\psi\,, & \text{in} \quad (0,l)\times(-a,a)\,,\\ \psi(s,\pm a) = 0\,, & \forall s\in(0,l)\,,\\ \psi(0,t) = \psi(l,-t)\,, & \forall t\in(-a,a)\,,\\ \partial_1\psi(0,t) = \partial_1\psi(l,-t)\,, & \forall t\in(-a,a)\,. \end{cases} \tag{3.2}$$

This is also the eigenvalue problem $\tilde{H}\psi = \lambda\psi$ for the self–adjoint operator $\tilde{H}$ in $L^2\left((0,l)\times(-a,a)\right)$ defined as

$$\begin{aligned} &\tilde{H}\psi := -\Delta\psi\\ &\mathrm{Dom}(\tilde{H}) := \Big\{\psi\in W^{2,2}\left((0,l)\times(-a,a)\right)\Big|\,\psi \text{ satisfies the boundary}\\ &\qquad\qquad\qquad\qquad\qquad\qquad\qquad\qquad\qquad\qquad \text{conditions of (3.2)}\Big\}. \end{aligned}$$

It is easy to check that $\tilde{H}\subset H$. As it is more convenient, let us work with $\tilde{H}$ for the moment. The spectrum of the operator $\tilde{H}$ can be found by considering the (extended) periodic problem

$$\begin{cases} -\Delta\phi = \mu\phi\,, & \text{in} \quad (-l,l)\times(-a,a)\,,\\ \phi(s,\pm a) = 0\,, & \forall s\in(-l,l)\,,\\ \phi(-l,t) = \phi(l,t)\,, & \forall t\in(-a,a)\,,\\ \partial_1\phi(-l,t) = \partial_1\phi(l,t)\,, & \forall t\in(-a,a)\,. \end{cases} \tag{3.3}$$

More precisely, (3.3) is the eigenvalue problem $T\phi = \mu\phi$ for the self–adjoint operator T in an extended Hilbert space $L^2\left((-l,l)\times(-a,a)\right)$ defined as

$$\begin{aligned} &T\phi := -\Delta\phi\,,\\ &\mathrm{Dom}(T) := \Big\{\phi\in W^{2,2}((-l,l)\times(-a,a))\Big|\,\phi \text{ satisfies the boundary}\\ &\qquad\qquad\qquad\qquad\qquad\qquad\qquad\qquad\qquad\qquad \text{conditions of (3.3)}\Big\}. \end{aligned}$$

This problem can be solved by separation of variables and the spectrum of T is well known in the form

$$\sigma(T) = \left\{\left(\frac{m\pi}{l}\right)^2 + \left(\frac{n\pi}{2a}\right)^2\right\}_{m\in\mathbb{Z},n\in\mathbb{N}},$$

where the convention $\mathbb{N} = \{1, 2, \dots\}$ is used. The corresponding eigenfunctions of T are

$$\phi_{m,n} = \varphi_m(s)\chi_n(t),$$

where

$$\varphi_m(s) := \sqrt{\frac{1}{2l}}\, e^{i\frac{\pi}{l}ms}\,, \qquad \chi_n(t) := \begin{cases} \sqrt{\frac{1}{a}}\,\cos(\frac{n\pi}{2a}t) & \text{if } n \text{ is odd}\,, \\ \sqrt{\frac{1}{a}}\,\sin(\frac{n\pi}{2a}t) & \text{if } n \text{ is even}\,. \end{cases}$$

The eigenfunctions $\{\phi_{m,n}\}_{m\in\mathbb{Z},n\in\mathbb{N}}$ of the self–adjoint operator T also form a complete orthonormal set in $L^2\left((-l,l)\times(-a,a)\right)$ (see [4]). By symmetry properties of φ_m and χ_n, we have

$$\begin{aligned} \phi_{m,n}(l,-t) &= (-1)^{m+n+1}\,\phi_{m,n}(0,t)\,, \\ \partial_1\phi_{m,n}(l,-t) &= (-1)^{m+n+1}\,\partial_1\phi_{m,n}(0,t)\,. \end{aligned}$$

Thus $\phi_{m,n}$ satisfies the boundary conditions of (3.2) if, and only if, $m+n$ is odd. Consequently,

$$\sigma(\tilde{H}) \supset \left\{ \left(\frac{m\pi}{l}\right)^2 + \left(\frac{n\pi}{2a}\right)^2 \right\}_{m\in\mathbb{Z},\ n\in\mathbb{N},\ m+n \text{ is odd}} \tag{3.4}$$

and the corresponding normalised eigenfunctions of $\tilde{H}$ are given by the restrictions

$$\psi_{m,n} := \sqrt{2}\,\phi_{m,n} \restriction (0,l)\times(-a,a)\,, \qquad m\in\mathbb{Z},\ n\in\mathbb{N},\ m+n \text{ is odd}\,.$$

To show that the right-hand side of (3.4) determines *all* the eigenvalues of $\tilde{H}$, we need the following result.

Proposition 1. $\{\psi_{m,n}\}_{m\in\mathbb{Z},\ n\in\mathbb{N},\ m+n \text{ is odd}}$ is a complete orthonormal set in $L^2((0,l)\times(-a,a))$.

Proof. The property that $\{\phi_{m,n}\}_{m\in\mathbb{Z},\ n\in\mathbb{N}}$ is a complete orthonormal set in $L^2((-l,l)\times(-a,a))$ is equivalent to the validity of the Parseval equality

$$\|f\|^2 = \sum_{m\in\mathbb{Z},\,n\in\mathbb{N}} |(\phi_{m,n}, f)|^2 \tag{3.5}$$

for every $f\in L^2((-l,l)\times(-a,a))$. Given an arbitrary $g\in L^2((0,l)\times(-a,a))$, we define the extension

$$f(s,t) := \begin{cases} g(s,t) & \text{if} \quad s>0\,, \\ g(s+l,-t) & \text{if} \quad s<0\,. \end{cases}$$

By an obvious integral substitution, it is straightforward to check the identity

$$\|f\|^2 = 2\,\|g\|^2\,. \tag{3.6}$$

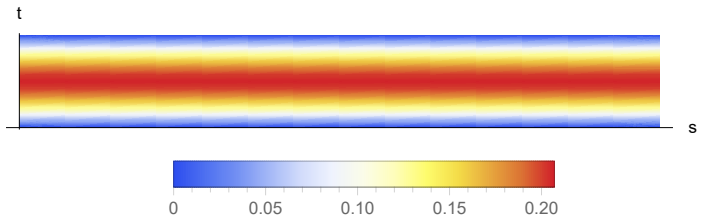

Figure 3.4: A plot of $\psi_{0,1}$, the eigenfunction corresponding to the lowest eigenvalue of the fake Möbius strip with $R = \frac{18}{2\pi}$ and $a = 1.3$.

At the same time, using in addition to the substitution the symmetry properties of φ_m and χ_n, we have

$$(\phi_{m,n}, f) = \frac{1}{\sqrt{2}} \left[1 + (-1)^{m+n+1}\right] (\psi_{m,n}, g)\,. \tag{3.7}$$

Putting (3.6) and (3.7) into (3.5), we get the Parseval inequality

$$\|g\|^2 = \sum_{\substack{m\in\mathbb{Z},\, n\in\mathbb{N} \\ m+n \text{ is odd}}} |(\psi_{m,n}, g)|^2\,,$$

which is equivalent to the desired completeness result. □

As a consequence of this proposition, we conclude with the result

$$\sigma(\tilde{H}) = \left\{ \left(\frac{m\pi}{l}\right)^2 + \left(\frac{n\pi}{2a}\right)^2 \right\}_{m\in\mathbb{Z},\ n\in\mathbb{N},\ m+n \text{ is odd}}\,. \tag{3.8}$$

However, as the found eigenfunctions of $\tilde{H}$ form a complete orthonormal set, we conclude that $\tilde{H} = H$ and indeed

$$\sigma(H) = \sigma(\tilde{H}) = \left\{ \left(\frac{m\pi}{l}\right)^2 + \left(\frac{n\pi}{2a}\right)^2 \right\}_{m\in\mathbb{Z},\ n\in\mathbb{N},\ m+n \text{ is odd}}\,.$$

Remark 3.1. The lowest eigenvalue

$$\lambda_{0,1} = \left(\frac{\pi}{2a}\right)^2$$

is simple and the corresponding eigenfunction $\psi_{0,1}$ (see Fig. 3.4) is positive. The eigenvalues $\lambda_{m,n}$ with $m \neq 0$ are always degenerate. In particular, this is true for the second eigenvalue

$$\min\{\lambda_{1,2} = \lambda_{-1,2}, \lambda_{2,1} = \lambda_{-2,1}\}.$$

Furthermore, if $l = 2a$ then the second eigenvalue $\frac{5\pi^2}{4a^2}$ has multiplicity *four*!

3.2 Not–so–fake Möbius strip

In this section, more realistic model of the Möbius strip is discussed. It arises from the fake strip, but we add the effective potential V_0 defined as

$$V_0(s,t) := -\frac{\pi^2}{2l^2}\cos(2\tfrac{\pi}{l}s)\,. \tag{3.9}$$

For a density plot of the potential, please see Fig. 3.5. Even though the model is still flat, the addition of V_0 makes it applicable to very narrow strips (when their width tends to zero). Rigorous proof of this claim can be found in Section 3.6.

Let us start with a quadratic form h_0

$$\begin{cases} h_0[\psi] := \displaystyle\int_{\Omega_0} |\nabla\psi|^2 \;+\; \int_{\Omega_0} V_0|\psi|^2 \;= h[\psi] + \int_{\Omega_0} V_0|\psi|^2\,, \\ \mathrm{Dom}(h_0) := \{\psi \in W^{1,2}(\Omega_0) \,\big|\, \psi(s,\pm a) = 0 \quad \forall s \in (0,l), \\ \qquad\qquad\qquad\qquad \psi(0,t) = \psi(l,-t) \quad \forall t \in (-a,a)\}\,. \end{cases}$$

We have already established that h is bounded from below and closed. Denoting $v_0[\psi] := \int_{\Omega_0} V_0|\psi|^2$, v_0 is a symmetric quadratic form. Moreover, it is relatively bounded with respect to h with the relative bound being 0, as

$$\begin{aligned} \mathrm{Dom}[h] \subset \mathrm{Dom}[v_0] &= L^2(\Omega_0) \\ |v_0[\psi]| = \left|\int_{\Omega_0} V_0|\psi|^2\right| &\le \frac{\pi^2}{2l^2}\|\psi\|^2\,. \end{aligned}$$

Then, by [38, Sec. VI.1.6], h_0 is bounded from below and closed, as well as densely defined. By the representation theorem ([38, Thm. VI.2.6]), the operator H_0

$$\begin{aligned} \mathrm{Dom}(H_0) &:= \{\psi \in \mathrm{Dom}(h_0) \,|\, \exists \eta \in \mathscr{H},\, \forall \phi \in \mathrm{Dom}(h_0),\, h_0(\phi,\psi) = (\phi,\eta)\}\,, \\ H_0\psi &:= \eta\,. \end{aligned}$$

associated with the form h_0 is bounded from below and self–adjoint.

Now consider the boundary value problem

$$\begin{cases} (-\Delta + V_0(s,t))\psi = \lambda\psi\,, & \text{in} \quad (0,l)\times(-a,a)\,, \\ \psi(s,\pm a) = 0\,, & \forall s \in (0,l)\,, \\ \psi(0,t) = \psi(l,-t)\,, & \forall t \in (-a,a)\,, \\ \partial_1\psi(0,t) = \partial_1\psi(l,-t)\,, & \forall t \in (-a,a)\,, \end{cases} \tag{3.10}$$

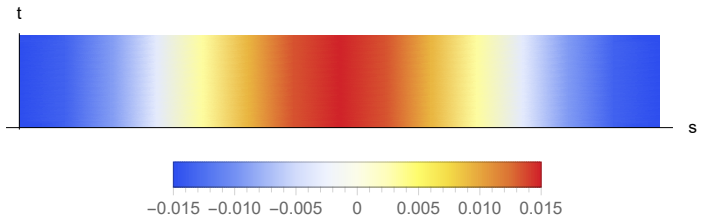

Figure 3.5: A density plot of the effective potential V_0 (see (3.9)) for the Möbius strip with width $2a = 2.6$ and length $l = 18$.

where l and a are arbitrary positive numbers and the potential V_0 is defined in (3.9). More precisely, (3.10) is the eigenvalue problem $\tilde{H}_0\psi = \lambda\psi$ for the self-adjoint operator $\tilde{H}_0$ in $L^2((0,l)\times(-a,a))$ defined as follows:

$$\begin{aligned}\tilde{H}_0\psi &:= (-\Delta + V_0(s,t))\psi\,,\\ \mathrm{Dom}(\tilde{H}_0) &:= \Big\{\psi \in W^{2,2}((0,l)\times(-a,a)) \Big| \psi \text{ satisfies the boundary conditions of (3.10)}\Big\}.\end{aligned}$$

Again, $\tilde{H}_0 \subset H_0$ and we consider the spectral problem of operator $\tilde{H}_0$ first for convenience. The spectrum of $\tilde{H}_0$ can be found once more by considering the periodic problem

$$\begin{cases} (-\Delta + V_0(s,t))\phi = \zeta\phi\,, & \text{in} \quad (-l,l)\times(-a,a)\,,\\ \phi(s,\pm a) = 0\,, & \forall s \in (-l,l)\,,\\ \phi(-l,t) = \phi(l,t)\,, & \forall t \in (-a,a)\,,\\ \partial_1\phi(-l,t) = \partial_1\phi(l,t)\,, & \forall t \in (-a,a)\,. \end{cases} \tag{3.11}$$

More precisely, (3.11) is the eigenvalue problem $S\phi = \zeta\phi$ for the self-adjoint operator S in an extended Hilbert space $L^2((-l,l)\times(-a,a))$ defined as

$$\begin{aligned}S\phi &:= (-\Delta + V_0(s,t))\phi\,,\\ \mathrm{Dom}(S) &:= \Big\{\phi \in W^{2,2}((-l,l)\times(-a,a)) \Big| \phi \text{ satisfies the boundary conditions of (3.11)}\Big\}.\end{aligned}$$

The eigenvalues and eigenfunctions of S can be found by separation of variables. In the variable t we get the same result as in the previous section. The normalised eigenfunctions of $-\frac{\mathrm{d}^2}{\mathrm{d}t^2}$ in $L^2((-a,a),\mathrm{d}t)$ with Dirichlet boundary conditions are numbered by $n \in \mathbb{N}$ and given by

$$\chi_n(t) := \begin{cases} \sqrt{\frac{1}{a}}\cos(\frac{n\pi}{2a}t) & \text{if } n \text{ is odd}\,,\\ \sqrt{\frac{1}{a}}\sin(\frac{n\pi}{2a}t) & \text{if } n \text{ is even}\,. \end{cases}$$

The corresponding eigenvalues are

$$\left(\frac{n\pi}{2a}\right)^2, \quad n \in \mathbb{N}.$$

The case of the second variable s is a little bit more involved. After the separation, we arrive at the following differential equation

$$-\varphi''(s) - \frac{\pi^2}{2l^2}\cos\left(\frac{2\pi}{l}s\right)\varphi(s) = \nu\varphi(s)\,. \tag{3.12}$$

It turns out that this is the Mathieu differential equation. Before we proceed any further let us first review basic properties of Mathieu functions.

Remark 3.2 (Mathieu functions). We use the following notation (see also [12]). Fix $q, \mu \in \mathbb{R}$ and consider the ordinary differential equation

$$y''(\eta) + (\mu - 2q\cos(2\eta))y(\eta) = 0\,. \tag{3.13}$$

This equation has a 2π-periodic solution if and only if $\mu = a_r(q)$ or $\mu = b_r(q)$, where $a_r(q)$, $r \in \mathbb{N}_0$, and $b_r(q)$, $r \in \mathbb{N}$, are the so called Mathieu characteristic values. These characteristic values satisfy

$$\begin{aligned} &q > 0: \ a_0 < b_1 < a_1 < b_2 < a_2 < \cdots\,, \\ &q < 0: \ a_0 < a_1 < b_1 < b_2 < a_2 < \cdots\,, \\ &q = 0: \ a_r(0) = b_r(0) = r^2\,. \end{aligned} \tag{3.14}$$

The Mathieu integral order functions $\mathrm{ce}_r(\eta, q)$, $r \in \mathbb{N}_0$, and $\mathrm{se}_r(\eta, q)$, $r \in \mathbb{N}$, are defined in the following way: $\mathrm{ce}_r(\eta, q)$ is the even solution of (3.13) with $\mu = a_r(q)$ and $\mathrm{se}_r(\eta, q)$ is the odd solution of (3.13) with $\mu = b_r(q)$. Both $\mathrm{ce}_r(\cdot, q)$ and $\mathrm{se}_r(\cdot, q)$ are 2π-periodic. Moreover, $\mathrm{ce}_{2r}(\cdot, q)$ and $\mathrm{se}_{2r+2}(\cdot, q)$ are π-periodic and $\mathrm{ce}_{2r+1}(\cdot, q)$ and $\mathrm{se}_{2r+1}(\cdot, q)$ are antiperiodic with antiperiod π. For any $q \in \mathbb{R}$, the integral order Mathieu functions $\mathrm{ce}_r(\eta, q)$ and $\mathrm{se}_r(\eta, q)$ taken together form an orthogonal basis in $L^2((-\pi, \pi), \mathrm{d}\eta)$ (see [1, §20.5]).

We assume both $\mathrm{ce}_r(\eta, q)$ and $\mathrm{se}_r(\eta, q)$ are normalised to $\sqrt{\pi}$ in $L^2((-\pi, \pi), \mathrm{d}\eta)$, *i.e.* the equalities

$$\int_{-\pi}^{\pi} |\,\mathrm{ce}_r(\eta, q)|^2\,\mathrm{d}\eta = \int_{-\pi}^{\pi} |\,\mathrm{se}_r(\eta, q)|^2\,\mathrm{d}\eta = \pi$$

hold for all possible values of r. This convention is in agreement with [12] and it is respected by *Mathematica*, too. The (anti)periodicity then implies

$$\int_{0}^{\pi} |\,\mathrm{ce}_r(\eta, q)|^2\,\mathrm{d}\eta = \int_{0}^{\pi} |\,\mathrm{se}_r(\eta, q)|^2\,\mathrm{d}\eta = \frac{\pi}{2}\,.$$

Let us return to the equation (3.12). Employing a simple change of the independent variable, $\eta = \frac{\pi}{l}s$, we immediately get the Mathieu equation (3.13) (with $q = -\frac{1}{4}$ and $\mu = \frac{l^2}{\pi^2}\nu$). Thus the equation (3.12) has the following $2l$-periodic and normalised solutions if and only if ν satisfies one of the

indicated conditions

$$\varphi_r^{(1)}(s) := \frac{1}{\sqrt{\pi}}\,\mathrm{se}_r\left(\frac{\pi}{l}s, -\frac{1}{4}\right), \qquad \text{if } b_r\left(-\frac{1}{4}\right) = \frac{l^2}{\pi^2}\nu\,, \text{ for some } r \in \mathbb{N}\,, \tag{3.15}$$

$$\varphi_r^{(2)}(s) := \frac{1}{\sqrt{\pi}}\,\mathrm{ce}_r\left(\frac{\pi}{l}s, -\frac{1}{4}\right), \qquad \text{if } a_r\left(-\frac{1}{4}\right) = \frac{l^2}{\pi^2}\nu\,, \text{ for some } r \in \mathbb{N}_0\,. \tag{3.16}$$

The eigenvalues of S therefore are

$$\sigma(S) = \left\{\left(\frac{n\pi}{2a}\right)^2 + \frac{\pi^2}{l^2}a_r\left(-\frac{1}{4}\right)\right\}_{\substack{n\in\mathbb{N}\\ r\in\mathbb{N}_0}} \cup \left\{\left(\frac{n\pi}{2a}\right)^2 + \frac{\pi^2}{l^2}b_r\left(-\frac{1}{4}\right)\right\}_{\substack{n\in\mathbb{N}\\ r\in\mathbb{N}}}.$$

The corresponding normalised eigenfunctions form an orthogonal basis of $L^2((-l,l)\times(-a,a),\,\mathrm{d}s\,\mathrm{d}t)$,

$$\begin{aligned}\phi_{r,n}^{(1)}(s,t) &:= \varphi_r^{(1)}(s)\,\chi_n(t), \quad r\in\mathbb{N},\ n\in\mathbb{N},\\ \phi_{r,n}^{(2)}(s,t) &:= \varphi_r^{(2)}(s)\,\chi_n(t), \quad r\in\mathbb{N}_0,\ n\in\mathbb{N}.\end{aligned}$$

Let us now find the eigenfunctions and eigenvalues of the not–so–fake Möbius strip operator $\tilde{H}_0$. Note that for any $j = 1, 2$ the functions $\varphi_r^{(j)}$ are antiperiodic, resp. periodic, with antiperiod l, resp. period l, whenever r is odd, resp. even. Using this observation we establish the following key property of the eigenfunctions of S, namely

$$\begin{aligned}\phi_{r,n}^{(j)}(s+l,-t) &= \varphi_r^{(j)}(s+l)\cdot\chi_n(-t) = (-1)^r\varphi_r^{(j)}(s)\cdot(-1)^{n+1}\chi_n(t)\\ &= (-1)^{r+n+1}\phi_{r,n}^{(j)}(s,t)\,,\end{aligned} \tag{3.17}$$

for any $j = 1, 2$ and all permissible r and n. In particular, setting $s = 0$ in the last equation we have

$$\phi_{r,n}^{(j)}(l,-t) = (-1)^{r+n+1}\phi_{r,n}^{(j)}(0,t)\,.$$

and thus $\phi_{r,n}^{(j)}$, $j = 1, 2$, satisfies the boundary conditions of (3.10) if and only if $r + n$ is *odd*. Consequently,

$$\sigma(\tilde{H}_0) \supset \left\{\left(\frac{n\pi}{2a}\right)^2 + \frac{\pi^2}{l^2}a_r\left(-\frac{1}{4}\right)\right\}_{\substack{n\in\mathbb{N}\\ r\in\mathbb{N}_0\\ n+r\,\text{odd}}} \cup \left\{\left(\frac{n\pi}{2a}\right)^2 + \frac{\pi^2}{l^2}b_r\left(-\frac{1}{4}\right)\right\}_{\substack{n\in\mathbb{N}\\ r\in\mathbb{N}\\ n+r\,\text{odd}}}, \tag{3.18}$$

and the corresponding normalised eigenfunctions of $\tilde{H}_0$ are given by the restrictions

$$\psi_{r,n}^{(j)} := \sqrt{2}\,\phi_{r,n}^{(j)} \restriction (0,l)\times(-a,a)$$

where $(r,n) \in \mathbb{N}\times\mathbb{N}$ if $j = 1$ and $(r,n) \in \mathbb{N}_0\times\mathbb{N}$ if $j = 2$. That the normalisation factor $\sqrt{2}$ is correct follows from the final equations in Remark 3.2 and equations (3.15) and (3.16). For an illustration of how the $\varphi^{(j)}$ look like, please refer to the Fig. 3.6.

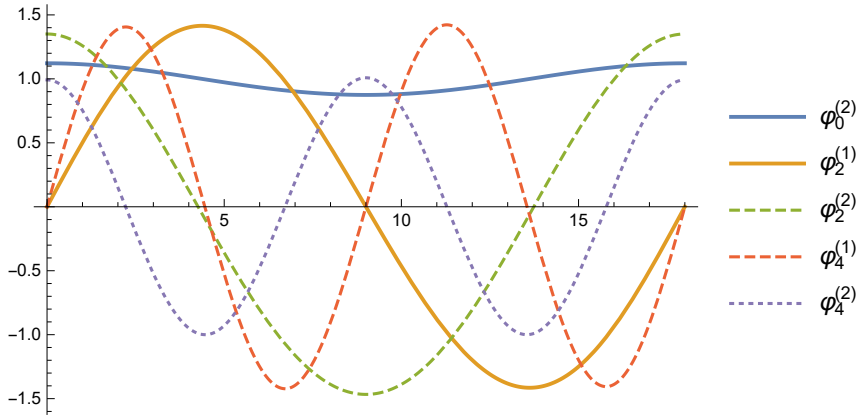

Figure 3.6: Illustration of the longitudinal parts, *i.e.* $\varphi^{(j)}$, of the first five eigenfunctions for the not–so–fake Möbius strip of length $l = 18$ and width $2a = 2.6$.

The kind reader surely feels an awkwardness in the last paragraph. Before we proceed any further let us therefore try to simplify our notation by putting

$$\mathbb{N}_1 := \mathbb{N} \times \mathbb{N} \quad \text{and} \quad \mathbb{N}_2 := \mathbb{N}_0 \times \mathbb{N}\,.$$

To show that the right-hand side of (3.18) determines *all* the eigenvalues of $\tilde{H}_0$, we need the following result analogous to Proposition 1.

Proposition 2. $\{\psi_{r,n}^{(j)}\}_{j=1,2,\,(r,n)\in\mathbb{N}_j,\,r+n\ is\ odd}$ is a complete orthonormal set in $L^2((0,l)\times(-a,a))$.

Proof. The property that the set $\{\phi_{r,n}^{(j)}\}_{j=1,2,\,(r,n)\in\mathbb{N}_j}$ is a complete orthonormal set in $L^2((-l,l)\times(-a,a))$ is equivalent to the validity of the Parseval equality

$$\|f\|^2 = \sum_{j=1,2,\,(r,n)\in\mathbb{N}_j} \left|(\phi_{r,n}^{(j)}, f)\right|^2 \tag{3.19}$$

for every $f \in L^2((-l,l)\times(-a,a))$. Given an arbitrary $g \in L^2((0,l)\times(-a,a))$, we define the extension $f \in L^2((-l,l)\times(-a,a))$ by

$$f(s,t) := \begin{cases} g(s,t) & \text{if} \quad s > 0\,, \\ g(s+l,-t) & \text{if} \quad s < 0\,. \end{cases}$$

By an obvious integral substitution, it is straightforward to check the identity

$$\|f\|^2 = 2\,\|g\|^2\,. \tag{3.20}$$

At the same time, using in addition to the substitution the symmetry prop-

erty (3.17) we have

$$\begin{aligned}(\phi^{(j)}_{r,n},\, f) &= \int_{(-l,0)\times(-a,a)} \phi^{(j)}_{r,n}(s,t) g(s+l,-t)\,\mathrm{d}s\mathrm{d}t \\ &\quad + \int_{(0,l)\times(-a,a)} \phi^{(j)}_{r,n}(s,t) g(s,t)\,\mathrm{d}s\mathrm{d}t \\ &= \int_{(0,l)\times(-a,a)} \phi^{(j)}_{r,n}(s-l,-t) g(s,t)\,\mathrm{d}s\mathrm{d}t \\ &\quad + \frac{1}{\sqrt{2}} \int_{(0,l)\times(-a,a)} \psi^{(j)}_{r,n}(s,t) g(s,t)\,\mathrm{d}s\mathrm{d}t \\ &= \frac{(-1)^{r+n+1}}{\sqrt{2}} \int_{(0,l)\times(-a,a)} \psi^{(j)}_{r,n}(s,t) g(s,t)\,\mathrm{d}s\mathrm{d}t \\ &\quad + \frac{1}{\sqrt{2}} \int_{(0,l)\times(-a,a)} \psi^{(j)}_{r,n}(s,t) g(s,t)\,\mathrm{d}s\mathrm{d}t \\ &= \frac{1}{\sqrt{2}} \big((-1)^{r+n+1}+1\big)(\psi^{(j)}_{r,n},\, g)\,. \end{aligned} \tag{3.21}$$

Putting (3.20) and (3.21) into (3.19), we get the Parseval inequality

$$\|g\|^2 = \sum_{\substack{j=1,2,\,(r,n)\in\mathbb{N}_j \\ r+n \text{ is odd}}} \big|(\psi^{(j)}_{r,n},\, g)\big|^2\,,$$

which is equivalent to the desired completeness result. □

As a consequence of this proposition, we conclude with the desired result $\tilde{H}_0 = H_0$ and the spectrum of H_0 reads

$$\sigma(H_0) = \left\{ \left(\frac{n\pi}{2a}\right)^2 + \frac{\pi^2}{l^2} a_r\left(-\frac{1}{4}\right) \right\}_{\substack{n\in\mathbb{N} \\ r\in\mathbb{N}_0 \\ n+r\,\text{odd}}} \cup \left\{ \left(\frac{n\pi}{2a}\right)^2 + \frac{\pi^2}{l^2} b_r\left(-\frac{1}{4}\right) \right\}_{\substack{n\in\mathbb{N} \\ r\in\mathbb{N} \\ n+r\,\text{odd}}}.$$

Remark 3.3. The smallest eigenvalue of the operator $H_0 = H + V_0$ is given by (indeed, note equations (3.18) and (3.14))

$$\left(\frac{\pi}{2a}\right)^2 + \frac{\pi^2}{l^2} a_0\left(-\frac{1}{4}\right).$$

Therefore, we get the estimate

$$\underbrace{\left(\frac{\pi}{2a}\right)^2}_{\lambda_{0,1}} + \frac{\pi^2}{l^2} a_0\left(-\frac{1}{4}\right) \le \lambda_{0,1}\,,$$

as (according to *Mathematica*)

$$\pi^2 a_0\left(-\frac{1}{4}\right) \approx -0.3063466\,.$$

3.3 Full Möbius strip

As stated beforehand, the full Möbius strip eluded our attempts at analytical solutions. Therefore, in this section, we only present the formal statement of the spectral problem as opposed to including the solutions as well. The numerical solutions are presented in a later section instead.

For the full model, we consider the following boundary value problem

$$\begin{cases} -\left(\frac{1}{f}\,\partial_1\,\frac{1}{f}\,\partial_1 - \frac{1}{f}\,\partial_2\,f\,\partial_2\right)\psi = \lambda\psi\,, & \text{in} \quad (0,l)\times(-a,a)\,, \\ \psi(s,\pm a) = 0\,, & \forall s\in(0,l)\,, \\ \psi(0,t) = \psi(l,-t)\,, & \forall t\in(-a,a)\,, \\ \partial_1\psi(0,t) = \partial_1\psi(l,-t)\,, & \forall t\in(-a,a)\,, \end{cases} \tag{3.22}$$

where f is defined in (3.1). Again, (3.22) is the eigenvalue problem $H_a\psi = \lambda\psi$ for the self–adjoint operator H_a in $L^2\left((0,l)\times(-a,a), f\,\mathrm{d}s\,\mathrm{d}t\right)$ defined as follows

$$H_a\psi := -\left(\frac{1}{f}\,\partial_1\,\frac{1}{f}\,\partial_1 - \frac{1}{f}\,\partial_2\,f\,\partial_2\right)\psi\,,$$

$$\mathrm{Dom}(H_a) := \Big\{\psi\in W^{2,2}((0,l)\times(-a,a))\Big|\,\psi \text{ satisfies the boundary conditions of (3.22)}\Big\}.$$

3.4 Numerical prerequisites

This section serves as a brief review of some basic approaches of numerical mathematics used in our study of the spectrum of the Laplace–Beltrami operator on the Möbius strip with various boundary conditions. As this thesis is not primarily concerned with the topic of programming and numerical solutions, the goal of this text is to provide only a short recollection of the utilized procedures.

Out of the numerous ways how one can (at least) numerically solve partial differential equations, we elected for the Finite Difference Method (FDM). This procedure is based on substituting the derivatives with their respective finite differences. In other words, the problem of finding solutions to the partial differential equation is converted to a much easier problem of solving a system of linear algebraic equations.

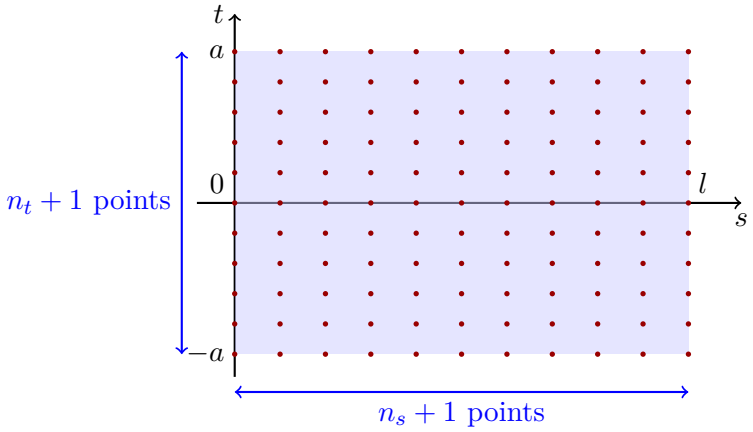

Figure 3.7: Rectangular grid formed by $(n_t + 1) \cdot (n_s + 1)$ points from the strip $(0, l) \times (-a, a)$.

Let us consider only a one–dimensional example for the moment. Be $u : (a, b) \to \mathbb{R}$ a differentiable function. Then in the FDM, the first derivative of u can be approximated using various finite differences:

$$\begin{aligned} &\text{forward difference:} && u'(x) \approx \frac{u(x+h) - u(x)}{h}\,, \\ &\text{symmetric difference:} && u'(x) \approx \frac{u(x+h) - u(x-h)}{2h}\,, \\ &\text{backward difference:} && u'(x) \approx \frac{u(x) - u(x-h)}{h}\,. \end{aligned}$$

Each differences can be useful in a different situation. The second derivative, u'', is usually replaced by the following expression

$$u''(x) \approx \frac{u(x+h) - 2u(x) + u(x-h)}{h^2},$$

which is obtained by combining the forward and backward difference for the first derivative and then using the symmetric one.

Applying this procedure to higher–dimensional problems, the differences are done in each variable separately, *i.e.* (using the forward difference)

$$\psi_{,s}(s,t) \approx \frac{\psi(s+h,t) - \psi(s,t)}{h}\,.$$

Normally, the discretization is based on a simple rectangular grid (see Fig. 3.7). However, this approach was found unsuitable for our model of the full Möbius strip, which can be found in this chapter, due to the nodes at the seam and their subsequent glueing. The resulting matrices were not symmetric, which considerably complicated the numerical algorithms, resulting in some imaginary numerical residues in the spectrum. We therefore implemented

another discretization scheme, which circumvents this problem by shifting all the nodes in the s direction by a half of the difference, $\frac{ds}{2}$. The resulting shifted grid can be found on Fig. 3.8. This, together with fine choosing from the possible differences, secured the correct execution of the computation.

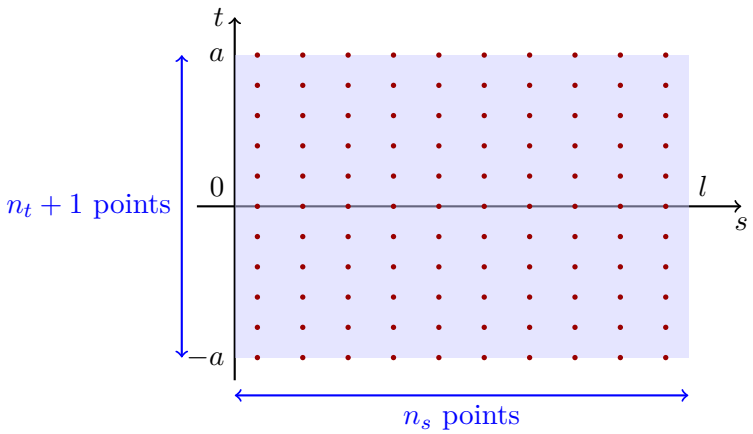

Figure 3.8: Rectangular shifted grid formed by $(n_t + 1) \cdot n_s$ points from the strip $(0, l) \times (-a, a)$.

After converting the partial differential problem to simple algebraic equations, the operator in question is effectively replaced by a matrix operator acting in the vector space $\mathbb{C}^N$ (with potentially large N), the solutions being vectors from there. Increasing the number of points for discretization, that is by enhancing the resolution of the discretization, promises the numerical solutions to approach the original ones as the differences are closer to the actual value of the derivatives. This effect is demonstrated in the following section.

3.5 Numerical experiments

In this section, we present results of our numerical experiments. In order to find a numerical approximation to the eigenvalues of operators H, H_0 and H_a, we employ the finite difference discretization of the operator in question as stated in the previous section. As already discussed there, the discretization is based on a simple, resp. shifted, rectangular grid (see Figures 3.7 and 3.8). Additionally, the finer the grid is, the better approximation of the original spectrum we are expected to get. This effect is demonstrated in Figure 3.9 (fake Möbius) and Figure 3.10 (not–so–fake Möbius). As the spectrum of the full Möbius strip cannot be found analytically, we are unable to present such comparison. Nevertheless, we present at least the asymptotic behaviour in Fig 3.11. As we claim that the not–so–fake model is a reasonably good

approximation for narrow strips, the comparison of the respective eigenvalues is presented in Fig. 3.15.

As for the eigenfunctions, the comparison of the first three can be found in Fig. 3.12 and Fig. 3.13 for the fake vs. not–so–fake and not–so–fake vs. full model respectively.

Please note that all results are computed for our special choice of a Möbius strip with length $l = 18$ and width $2a = 2.6$. To obtain the spectrum for different values of length and width, the whole process needs to be repeated as the eigenvalues are not easily scaled according to these parameters. The metric function f for a width $n2a$ and a length ml reads

$$f(s,t) = \sqrt{\left(1 - \frac{n}{m}\frac{a\tau}{R}\cos 2\pi\xi\right)^2 + \left(\frac{n}{m}\right)^2\left(\frac{a\tau}{2R}\right)^2},$$

for $\tau \in (-1, 1)$ and $\xi \in (0, 1)$. We can se that the scaling depends only on the ratio of the width and length, however, this dependence is not trivial.

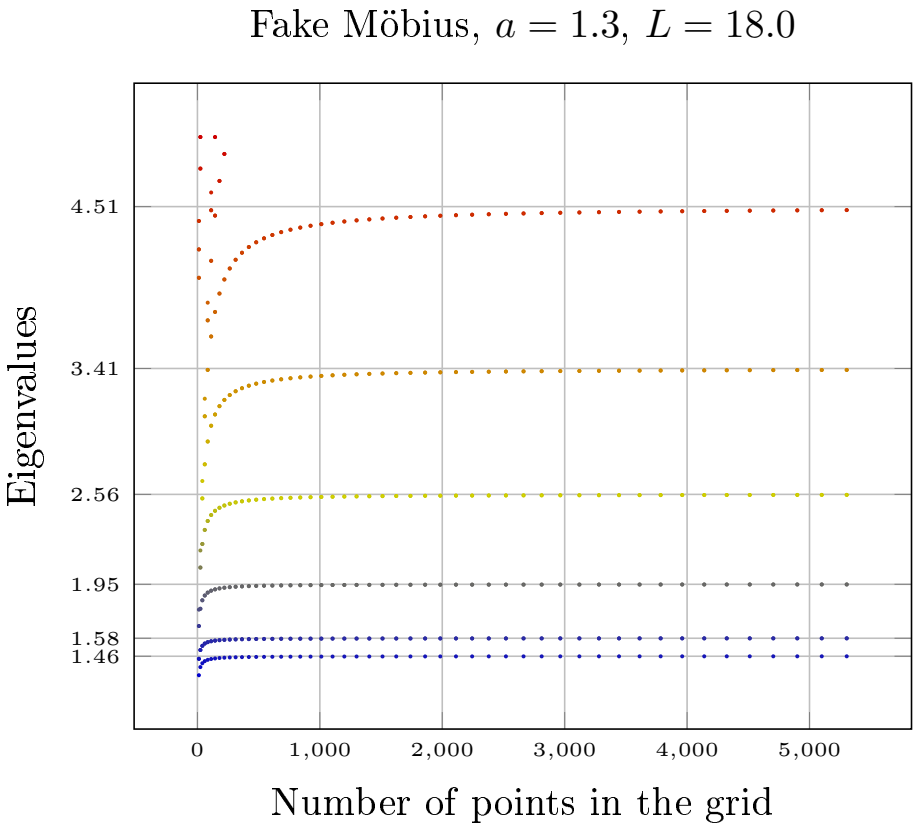

Figure 3.9: Graphical representation of the bottom of $\sigma(H)$ (fake Möbius) and its approximation by the finite difference method. We have chosen $a = 1.3$ and $l = 18$. The horizontal axis gives the size of the discretized matrix operator, which is related to the number of points in the grid $(n_t + 1) \cdot (n_s + 1)$ (we have taken $n_t = 2 + i$ and $n_s = 4 + 2i$ with $i = 1, 2, \ldots, 50$). Grey lines indicate the actual eigenvalues of H as given in (3.8)).

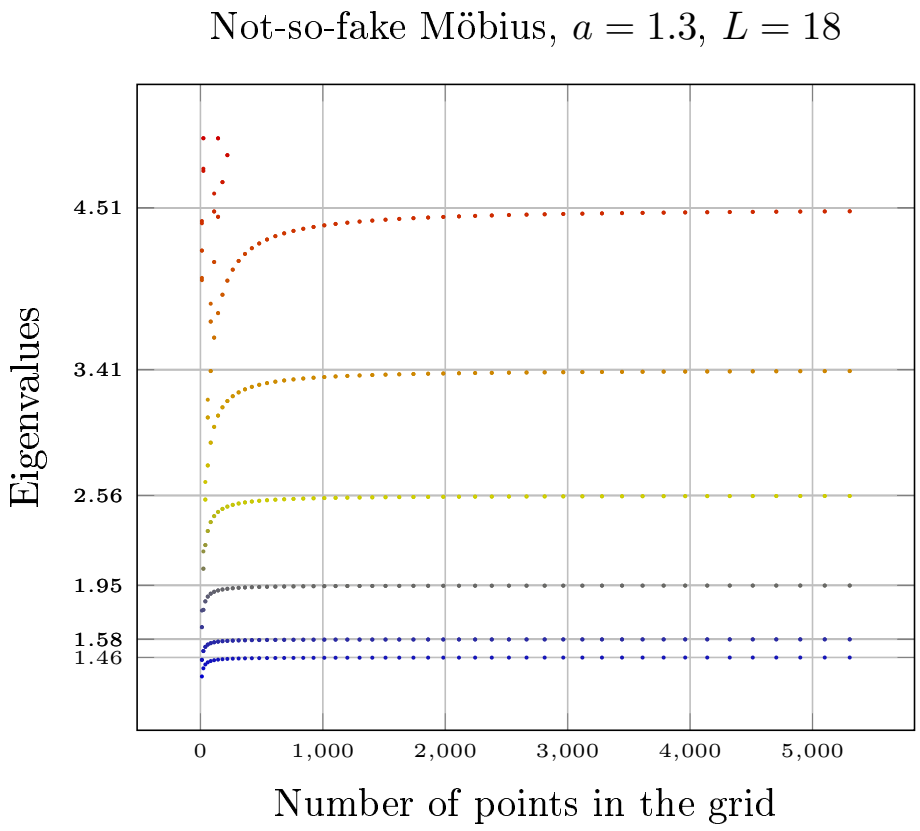

Figure 3.10: Graphical representation of the bottom of $\sigma(H_0)$ (not–so–fake Möbius) and its approximation by the finite difference method. We have chosen $a = 1.3$ and $l = 18$. The horizontal axis gives the size of the discretized matrix operator which is related to the number of points in the grid $(n_t + 1) \cdot (n_s + 1)$ (we have taken $n_t = 2 + i$ and $n_s = 4 + 2i$ with $i = 1, 2, \ldots, 50$). Grey lines indicate the actual eigenvalues of H_0 as given in (3.18)). As one can see on the left–hand side of the figure there are few very closely clustered eigenvalues (these are not degeneracies). From the picture, it is not obvious that the numerical result captures this effect correctly. Therefore, we present Table 3.1 where one can see the actual numerical values.

i	λ_1	λ_2	λ_3	λ_4	λ_5
1	1.33033	1.44221	1.44325	1.66392	1.66495
2	1.38548	1.50198	1.50298	1.78154	1.78154
3	1.41162	1.53030	1.53128	1.83916	1.83916
4	1.42598	1.54586	1.54683	1.87144	1.87144
5	1.43470	1.55530	1.55626	1.89124	1.89124
6	1.44038	1.56145	1.56241	1.90423	1.90423
7	1.44428	1.56568	1.56664	1.91321	1.91321
8	1.44708	1.56871	1.56967	1.91965	1.91965
9	1.44915	1.57096	1.57191	1.92444	1.92444
10	1.45073	1.57267	1.57362	1.9281	1.92810
11	1.45196	1.57400	1.57495	1.93094	1.93094
12	1.45293	1.57506	1.57601	1.93321	1.93321
13	1.45372	1.57591	1.57686	1.93504	1.93504
14	1.45437	1.57661	1.57756	1.93653	1.93653
15	1.45490	1.57719	1.57814	1.93778	1.93778
16	1.45535	1.57768	1.57862	1.93882	1.93882
17	1.45573	1.57809	1.57903	1.93970	1.93970
18	1.45605	1.57844	1.57938	1.94046	1.94046
19	1.45633	1.57874	1.57969	1.94111	1.94111
20	1.45657	1.57900	1.57995	1.94167	1.94167
21	1.45679	1.57923	1.58018	1.94216	1.94216
22	1.45697	1.57943	1.58038	1.94259	1.94259
23	1.45713	1.57961	1.58055	1.94297	1.94297
24	1.45728	1.57976	1.58071	1.94331	1.94331
25	1.45741	1.57990	1.58085	1.94361	1.94361
26	1.45752	1.58003	1.58098	1.94388	1.94388
27	1.45763	1.58014	1.58109	1.94412	1.94412
28	1.45772	1.58024	1.58119	1.94434	1.94434
29	1.45781	1.58033	1.58128	1.94454	1.94454
30	1.45788	1.58042	1.58136	1.94472	1.94472
31	1.45795	1.58049	1.58144	1.94488	1.94488
32	1.45802	1.58056	1.58151	1.94503	1.94503
33	1.45807	1.58063	1.58157	1.94516	1.94516
34	1.45813	1.58068	1.58163	1.94529	1.94529
35	1.45818	1.58074	1.58168	1.94540	1.94540
∞	1.45905514	1.58168901	1.58263442	1.94745194	1.94745204

Table 3.1: Five smallest eigenvalues of the operator H_0 (not–so–fake Möbius). We have chosen $a = 1.3$ and $l = 18$. The parameter i is related to the grid coarseness, in particular $n_t = 2 + i$ and $n_s = 4 + 2i$. The last row presents the exact value computed by Mathematica (see (3.18)). The values of λ_2 and λ_3, and λ_4 and λ_5, are indistinguishable in Figure 3.10.

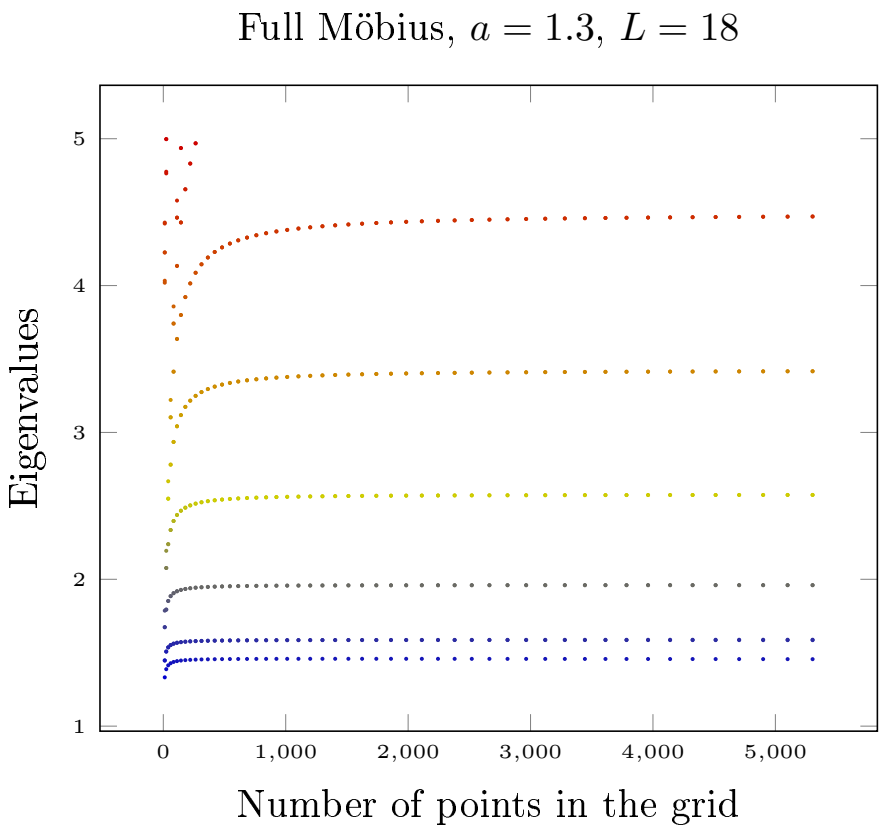

Figure 3.11: Graphical representation of the bottom of $\sigma(H_a)$ (full Möbius) and its approximation by the finite difference method. We have chosen $a = 1.3$ and $l = 18$. The horizontal axis gives the size of the discretized matrix operator which is related to the number of points in the grid $(n_t + 1) \cdot (n_s + 1)$ (we have taken $n_t = 2 + i$ and $n_s = 4 + 2i$ with $i = 1, 2, \ldots, 50$). As we do not know the exact value of the actual eigenvalues, there is no grey line visualising the wanted asymptotic behaviour. However, it is clear that the lowest eigenvalues converge.

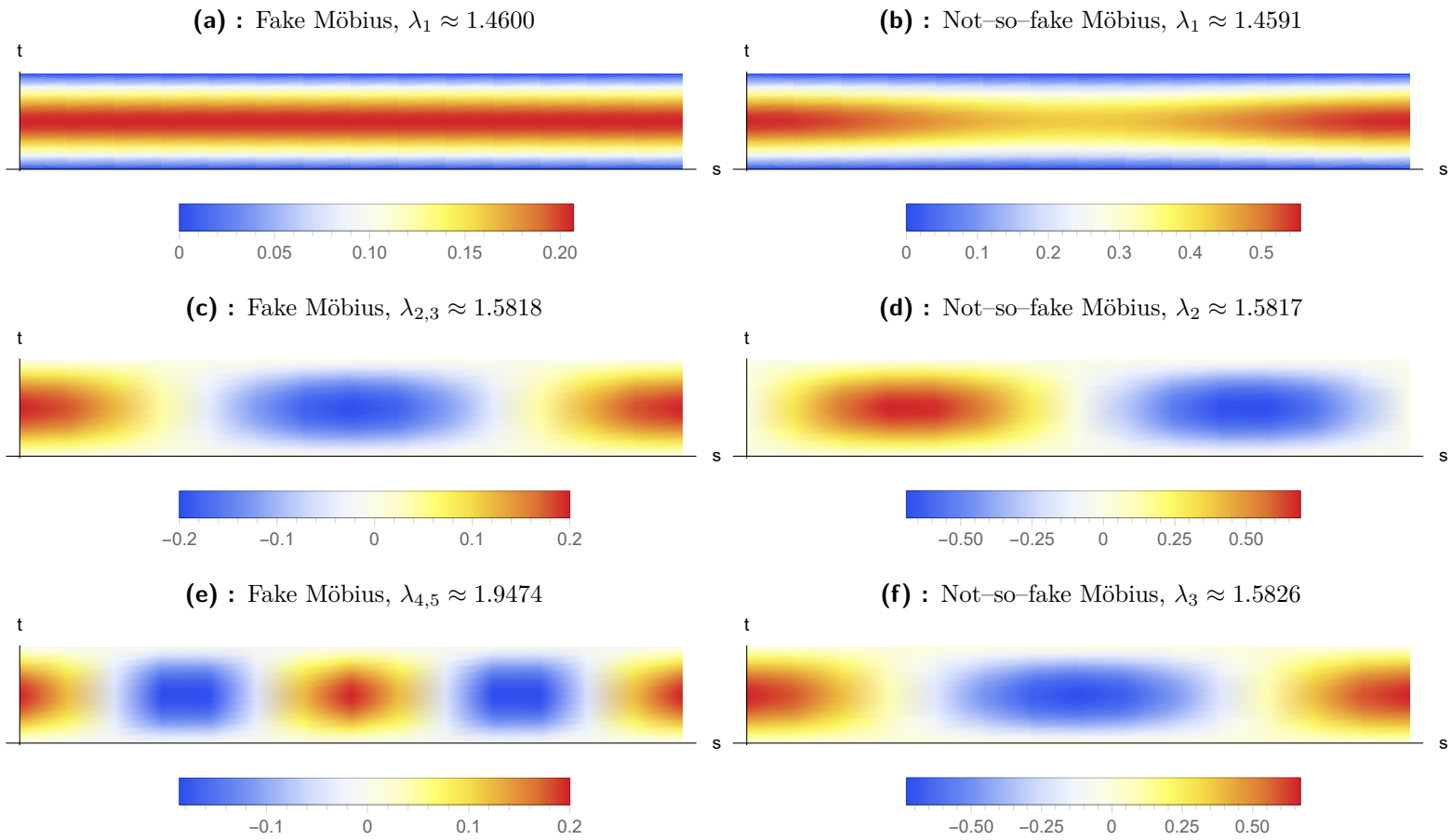

Figure 3.12: Plots comparing the first three eigenvectors of the fake Möbius strip and of the not–so–fake Möbius strip for the strip of width $a = 1.3$ with the length $l = 18$. For the fake model, all eigenvalues except the first are degenerate. However, it is not the case in the not–so–fake model, as the potential V_0 causes the degeneracy to disappear.

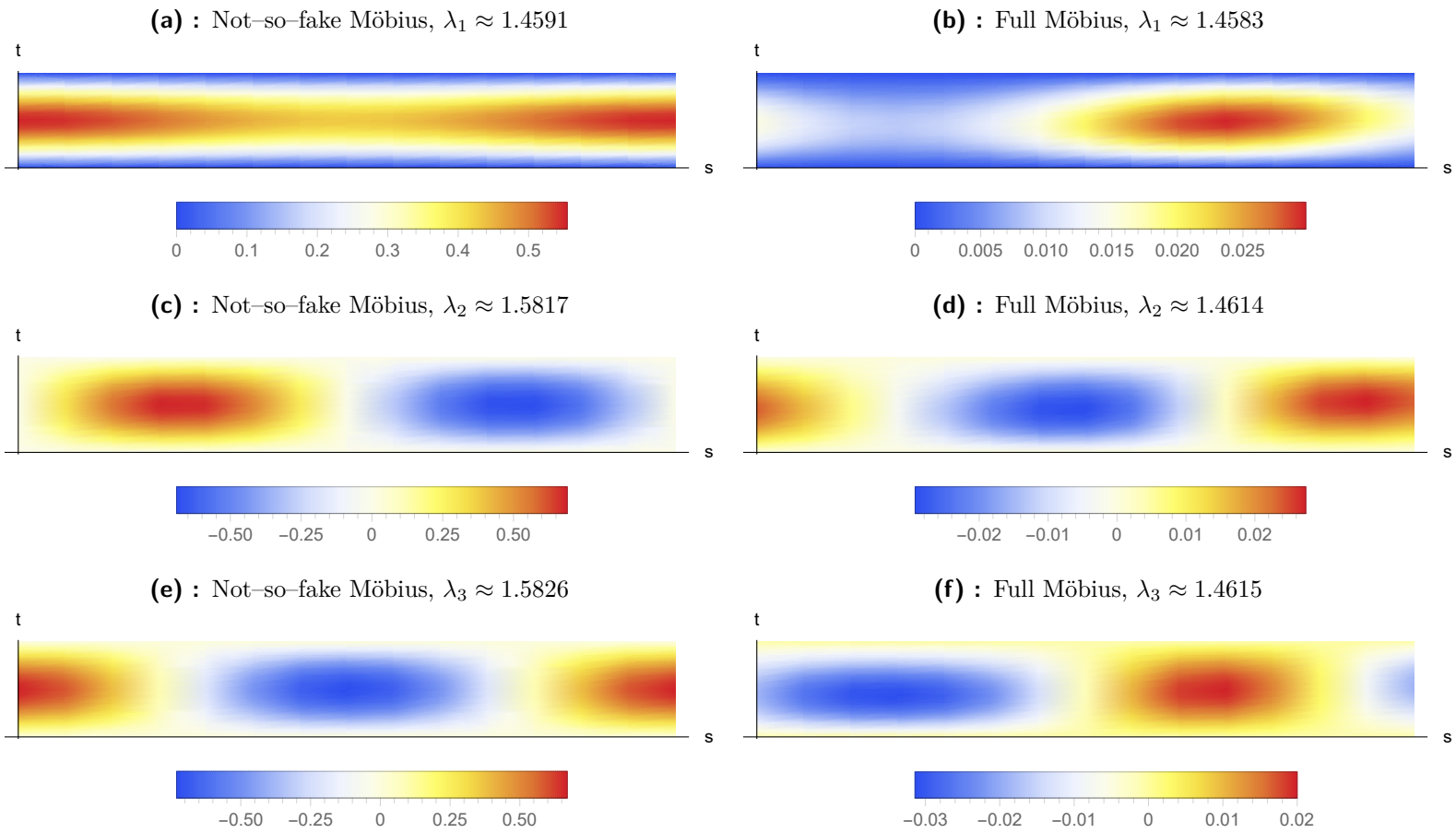

Figure 3.13: Plots comparing the first three eigenvectors of the not–so–fake Möbius strip (on the left) and of the full Möbius strip (on the right) for the strip of width $a = 1.3$ with the length $l = 18$.

(a) : First eigenfunction of the full Möbius, $\lambda_1 \approx 1.4583$

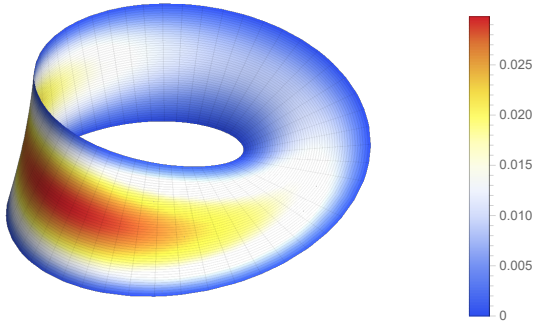

(b) : Second eigenfunction of the full Möbius, $\lambda_2 \approx 1.4614$

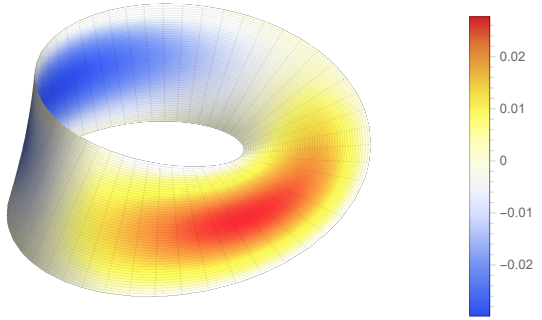

(c) : Third eigenfunction of the full Möbius, $\lambda_3 \approx 1.4614$

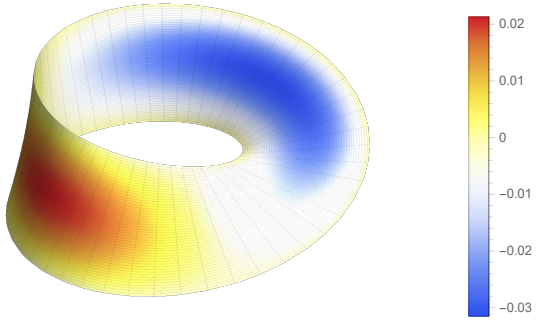

Figure 3.14: Visualization of the first three eigenfunctions of the full Möbius strip coiled on the actual strip.

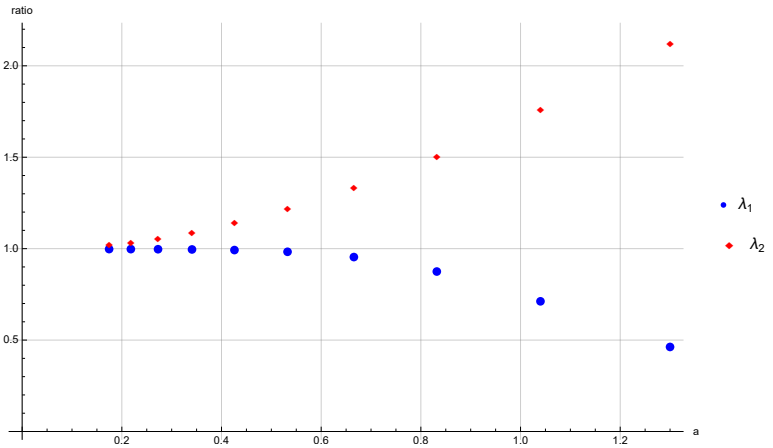

Figure 3.15: Plot of ratios of the first two computed eigenvalues of the full Möbius strip and the not–so–fake one for different widths of the strip of length $l = 18$. Clearly, the not–so–fake model is a good approximation of the full one for narrow ribbons.

3.6 Norm–resolvent convergence

In order to establish that the not–so–fake operator (3.10) is truly not so bad of an approximation of the full operator (3.22), we need to compare the two operators somehow. As the operators act on different Hilbert spaces, namely $\mathscr{H}_a' := L^2((0,l)\times(-a,a),\,\mathrm{d}s\,\mathrm{d}t)$ and $\mathscr{H}_a := L^2((0,l)\times(-a,a),\,f\,\mathrm{d}s\,\mathrm{d}t)$, we cannot compare them directly. Therefore, we employ the strategy of norm–resolvent convergence, as can be found in [34] or, in more abstract settings, in [31].

Firstly, we must utilize a unitary transformation U mapping $\mathscr{H}_a$ onto $\mathscr{H}_1 := L^2((0,l)\times(-1,1),\,\mathrm{d}s\,\mathrm{d}\tau)$,

$$U : \mathscr{H}_a \to \mathscr{H}_1\,,$$

operating such that

$$\phi(s,\tau) \equiv (U\psi)(s,\tau) := \sqrt{a}\sqrt{f(s,a\tau)}\psi(s,a\tau)\,,$$

where f is given by (3.1). For the not–so–fake model, it is enough the utilize the unitary transformation $U' : \mathscr{H}_a' \to \mathscr{H}_1$ given by

$$\phi(s,\tau) \equiv (U'\psi)(s,\tau) := \sqrt{a}\psi(s,a\tau)\,.$$

After these unitary transformations, the expression of the operators reads the following:

$$H_0' = -\partial_s^2 - \frac{1}{a^2}\partial_\tau + V_0\,, \tag{3.23}$$

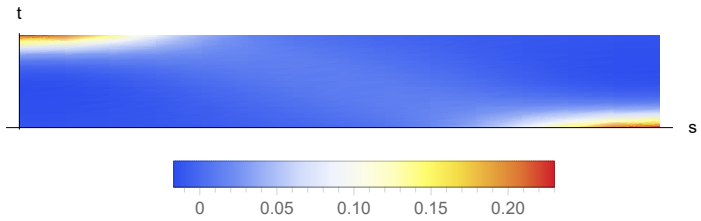

Figure 3.16: Density plot of the full potential V_a for the Möbius strip of length $l = 18$ and width $a = 2.6$.

for the not–so–fake case, with the potential V_0 being

$$V_0(s) := -\frac{\cos\frac{s}{R}}{8R^2}\,,$$

and

$$H_a' = -\partial_s \frac{1}{f^2}\partial_s - \frac{1}{a^2}\partial_\tau + V_a\,, \tag{3.24}$$

where the potential V_a can be written as

$$V_a = V_1 + V_2$$

with

$$\begin{aligned} V_1 = \Bigg[\left(2a^2t^2\cos\frac{s}{R} + 3a^2t^2 - 8atR\cos\frac{s}{2R} + 4R^2\right)^3\Bigg]^{-1} \\ \Bigg\{atR^3\left(48\cos\frac{s}{2R} + 16\cos\frac{3s}{2R}\right) \\ + a^3t^3R\left(98\cos\frac{s}{2R} + 24\cos\frac{3s}{2R} + 4\cos\frac{5s}{2R}\right) \\ - a^4t^4\left(\frac{67}{4} + 21\cos\frac{s}{R} + 3\cos\frac{2s}{R} + \frac{1}{2}\cos\frac{3s}{R}\right) \\ -a^2t^2R^2\left(67 + 60\cos\frac{s}{R} + 12\cos\frac{2s}{R}\right)\Bigg\} \end{aligned}$$

and

$$V_2 = \frac{8R^4\cos\frac{s}{R}}{\left(2a^2t^2\cos\frac{s}{R} + 3a^2t^2 - 8atR\cos\frac{s}{2R} + 4R^2\right)^3}\,.$$

This division is beneficial for capturing the behaviour of the different parts of the potential, as surely

$$\begin{aligned} V_1 &\overset{a\to 0}{\longrightarrow} 0\,, \\ V_2 - V_0 &\overset{a\to 0}{\longrightarrow} 0\,. \end{aligned}$$

To visualise the potential, please refer to the density plots of V_0 and V_a on Fig. 3.5 and Fig. 3.16 respectively.

In order to prove that H_0' approximates H_a' in a sense as $a \to 0$, we show that the difference of the respective resolvents tends to zero in operator norm.

Choosing some fixed $\zeta > 0$, we set

$$R := (H'_a + \zeta)^{-1}$$
$$R_0 := (H'_0 + \zeta)^{-1}.$$

Writing out the definition of the norm,

$$\|R - R_0\| = \sup_{F,G \in \mathscr{H}_1} \frac{|\,(F, (R - R_0)G)\,|}{\|F\|\|G\|}\,,$$

it is clear that it is enough to investigate the scalar product $(F, (R - R_0)G)$. Therefore we arrive at the following

$$(F, (R - R_0)G) = ((H'_0 + \zeta)\phi, \psi) - (\phi, (H'_a + \zeta)\psi) = h'_0(\phi, \psi) - h'_a(\phi, \psi)\,,$$

where

$$\phi := R_0 F\,,$$
$$\psi := R\,G\,,$$

and h'_0, h'_a are quadratic forms corresponding to the operators H'_0, H'_a. Calculating the difference of those quadratic forms, we get

$$\begin{aligned} h'_0(\phi, \psi) - h'_a(\phi, \psi) &= \int \bar{\phi}_{,s}\psi_{,s}\left(1 - \frac{1}{f^2}\right) \mathrm{d}s\,\mathrm{d}\tau + \int \bar{\phi}\psi(V_0 - V_a)\,\mathrm{d}s\,\mathrm{d}\tau \\ &\leq \max\left\{\|1 - \frac{1}{f^2}\|_\infty, \|V_0 - V_a\|_\infty\right\}\left(\|\phi_{,s}\|\,\|\psi_{,s}\| + \|\phi\|\,\|\psi\|\right). \end{aligned}$$

Furthermore, we have the following upper bounds

$$\begin{aligned} \|\phi\| &\leq \frac{8R^2}{8\zeta R^2 - 1}\,\|F\| \\ \|\phi_{,s}\| &\leq \sqrt{\frac{8R^2}{8\zeta R^2 - 1}}\,\|F\| \\ \|\psi\| &\leq \frac{1}{\zeta + \frac{\frac{165}{4}a^4 - 126a^3R + 139a^2R^2 - 64aR^3 + 8R^4}{(5a^2 + 8aR + 4R^2)^3}}\,\|G\| \\ \|\psi_{,s}\| &\leq \sqrt{\frac{4R^2 + 8R + 5}{4R^2\left(\zeta + \frac{\frac{165}{4}a^4 - 126a^3R + 139a^2R^2 - 64aR^3 + 8R^4}{(5a^2 + 8aR + 4R^2)^3}\right)}}\,\|G\| \end{aligned}$$

meaning, that

$$\|R - R_0\| \leq \max\left\{\|1 - \frac{1}{f^2}\|_\infty, \|V_0 - V_a\|_\infty\right\} j\,,$$

with

$$j = \frac{8R^2 + \sqrt{(8R^2 + 16R + 10)(8R^2\zeta - 1)\left(\zeta + \frac{\frac{165}{4}a^4 - 126a^3R + 139a^2R^2 - 64aR^3 + 8R^4}{(5a^2 + 8aR + 4R^2)^3}\right)}}{(8R^2\zeta - 1)\left(\zeta + \frac{\frac{165}{4}a^4 - 126a^3R + 139a^2R^2 - 64aR^3 + 8R^4}{(5a^2 + 8aR + 4R^2)^3}\right)}\,.$$

As the term $\max\left\{\|1-\frac{1}{f^2}\|_\infty, \|V_0 - V_a\|_\infty\right\}$ goes to 0 with $a \to 0$ as $\mathcal{O}(a)$, the norm $\|R - R_0\| \to 0$ as requested. We therefore conclude that the not–so–fake model is a suitable approximation for the behaviour of very thin ribbons.

Let us finish with a statement which summarizes this section.

Theorem 3.4. *Let H_0', H_a' be defined as in* (3.23)*, resp.* (3.24)*. Then there exists a constant C such that for all $a < R$,*

$$\|(H_a' - \zeta)^{-1} - (H_0' - \zeta)^{-1}\| \leq a\, C$$

for some fixed $\zeta > 0$.

Conclusion

This thesis was dedicated to generalizing of several theorems about the spectral behaviour of the Laplace–Beltrami operator with Dirichlet boundary condition on quantum nanoribbons in arbitrary dimension as well as finding the spectrum of the (full) Möbius strip.

The first chapter includes a summary of the theoretical foundations needed for the study of the quantum nanoribbons. The necessary prerequisites as well as the actual construction of the waveguide is outlined there, followed by an example of the construction in three dimensions with its specifics, and concluded by an introduction of some used notation.

In the second chapter, we present the spectral results of this thesis. Firstly, the Hamiltonian is properly introduced as a bounded self–adjoint operator acting on the quantum ribbon. Next, the spectrum of an asymptotically flat strip is localised, with the result matching our expectation from the situation in three dimensions (see [28]). The theorem claiming the manifestation of bound states for purely bent strips is also analogous to the one already known in three dimensions. Lastly, Hardy inequalities, which arises in twisted strips, are discussed along with their sufficient conditions.

Finally, the last chapter contains both analytical and numerical solutions for three different model of the Möbis strip. The solutions for the two easier ones – the fake and not–so–fake model, which can be found analytically, are presented. For the last model of the full strip, which sadly eluded our attempts on finding an analytical solution, the numerical solutions are presented instead. Several different comparisons of all of the cases are executed throughout the

chapter, supporting our claim that the solely numerical solution of the full model is plausible. We conclude the chapter with proving that in the limit of a thin strip, the full model converges to the not–so–fake on in the norm–resolvent sense, which justifies the inclusion of the not–so–fake model in our discussion of the Möbius strip.

For future investigations, we leave open the question whether the sufficient conditions for the Hardy inequality are really necessary or not. Another possibility for investigation is regarding the scaling of the spectrum of the Möbius strip, as the numerical results presented here were calculated only for a particular choice of the strip and the scaling formula is not obvious.

Bibliography

[1] M. Abramowitz and I. A. Stegun. *Handbook of Mathematical Functions, With Formulas, Graphs, and Mathematical Tables*. Dover Publications, Inc., New York, NY, USA, 1974.

[2] Y. Avishai, D. Bessis, B. G. Giraud, and G. Mantica. Quantum bound states in open geometries. *Physical Review B*, 44(15):8028–8034, October 1991.

[3] R. L. Bishop. There is more than one way to frame a curve. *The American Mathematical Monthly*, 82(3):246, March 1975.

[4] J. Blank, P. Exner, and M. Havlíček. *Lineární operátory v kvantové fyzice*. Praha: Karolinum, 1993.

[5] D. Borisov, T. Ekholm, and H. Kovařík. Spectrum of the magnetic Schrödinger operator in a waveguide with combined boundary conditions. *Annales Henri Poincaré*, 6(2):327–342, April 2005.

[6] D. Borisov, P. Exner, and R. Gadyl'shin. Geometric coupling thresholds in a two-dimensional strip. *Journal of Mathematical Physics*, 43:6265–6278, 2002.

[7] J. P. Carini, J. T. Londergan, K. Mullen, and D. P. Murdock. Bound states and resonances in waveguides and quantum wires. *Physical Review B*, 46(23):15538–15541, December 1992.

[8] J. P. Carini, J. T. Londergan, K. Mullen, and D. P. Murdock. Multiple bound states in sharply bent waveguides. *Physical Review B*, 48(7):4503–4515, August 1993.

[9] G. Carron, P. Exner, and D. Krejčiřík. Topologically nontrivial quantum layers. *Journal of Mathematical Physics*, 45(2):774–784, February 2004.

[10] C. H. O. Chui and P. A. Pearce. Finitized Conformal Spectra of the Ising Model on the Klein Bottle and Möbius Strip. *Journal of Statistical Physics*, 107(5/6):1167–1205, 2002.

[11] J. Dittrich and J. Kříž. Bound states in straight quantum waveguides with combined boundary conditions. *Journal of Mathematical Physics*, 43:3892–3915, 2002.

[12] *NIST Digital Library of Mathematical Functions*. http://dlmf.nist.gov/, Release 1.0.15 of 2017-06-01. F. W. J. Olver, A. B. Olde Daalhuis, D. W. Lozier, B. I. Schneider, R. F. Boisvert, C. W. Clark, B. R. Miller and B. V. Saunders, eds.

[13] P. Duclos, P. Exner, and D. Krejčiřík. Bound states in curved quantum layers. *Communications in Mathematical Physics*, 223(1):13–28, September 2001.

[14] P. Duclos, P. Exner, and D. Krejčiřík. Locally curved quantum layers. *Ukrainian J. Phys.*, pages 595–601, 2000.

[15] P. Exner and P. Duclos. Curvature-induced bound states in quantum waveguides in two and three dimensions. *Review of Mathematical Physics*, 7:73–102, 1995.

[16] P. Exner and P. Šeba. Bound states in curved quantum waveguides. *Journal of Mathematical Physics*, 30(11):2574–2580, November 1989.

[17] P. Exner and A. Minakov. Curvature-induced bound states in Robin waveguides and their asymptotical properties. *Journal of Mathematical Physics*, 55(12):122101, December 2014.

[18] P. W. Fowler and L. W. Jenneskens. Geometric localisation in Möbius π systems. *Chemical Physics Letters*, 427(1-3):221–224, August 2006.

[19] P. Freitas and D. Krejčiřík. Waveguides with Combined Dirichlet and Robin Boundary Conditions. *Mathematical Physics, Analysis and Geometry*, 9(4):335–352, February 2007.

[20] Y. Gaididei, A. Goussev, V. P. Kravchuk, O. V. Pylypovskyi, J. M. Robbins, D. D. Sheka, V. Slastikov, and S. Vasylkevych. Magnetization in narrow ribbons: curvature effects. *Journal of Physics A: Mathematical and Theoretical*, 50(38):385401, September 2017.

[21] J. Goldstone and R. L. Jaffe. Bound states in twisting tubes. *Phys. Rev. B*, 45:14100–14107, 1992.

[22] J. Gravesen and M. Willatzen. Eigenstates of Möbius nanostructures including curvature effects. *Phys. Rev. A*, 72:032108, September 2005.

[23] Z. L. Guo, Z.R. Gong, H. Dong, and C. P. Sun. Möbius graphene strip as a topological insulator. *Physical Review B*, 80(19), November 2009.

[24] W. Klingenberg and D. Hoffman. *A course in differential geometry*. Graduate Texts in Mathematics. Springer, 1978.

[25] R. S. Krausshar. The Helmholtz Operator on Higher Dimensional Möbius Strips Embedded in $\mathbb{R}^4$. *Advances in Applied Clifford Algebras*, 22(3):745–755, July 2012.

[26] R. S. Krausshar. The Klein-Gordon Operator on Möbius Strip Domains and the Klein Bottle in $\mathbb{R}^n$. *Mathematical Physics, Analysis and Geometry*, 16(4):363–379, December 2013.

[27] D. Krejčiřík. Spectrum of the Laplacian in a narrow curved strip with combined Dirichlet and Neumann boundary conditions. *ESAIM: Control, Optimisation and Calculus of Variations*, 15(3):555–568, May 2008.

[28] D. Krejčiřík and J. Kříž. On the spectrum of curved planar waveguides. *Publications of the Research Institute for Mathematical Sciences*, 41(3):757–791, 2005.

[29] D. Krejčiřík and Z. Lu. Location of the essential spectrum in curved quantum layers. *Journal of Mathematical Physics*, 55(8):083520, August 2014.

[30] D. Krejčiřík and N. Raymond. Magnetic effects in curved quantum waveguides. *Annales Henri Poincaré*, 15(10):1993–2024, December 2013.

[31] D. Krejčiřík, N. Raymond, J. Royer, and P. Siegl. Reduction of dimension as a consequence of norm-resolvent convergence and applications. *Mathematika*, 64(02):406–429, 2018.

[32] D. Krejčiřík. Quantum strips on surfaces. *Journal of Geometry and Physics*, 45:203–217, February 2003.

[33] D. Krejčiřík. Hardy inequalities in strips on ruled surfaces. *Journal of Inequalities and Applications*, November 2005.

[34] D. Krejčiřík and H. Šediváková. The Effective Hamiltonian in Curved Quantum Waveguides Under Mild Regularity Assumptions. *Reviews in Mathematical Physics*, 24:1250018, August 2012.

[35] P. Li and Z. Zhang. Continuous-time quantum walks on nonorientable surfaces: analytical solutions for Möbius strips and Klein bottles. *Journal of Physics A: Mathematical and Theoretical*, 45(28):285301, June 2012.

[36] R. Novák. Bound states in waveguides with complex Robin boundary conditions. *Asymptotic Analysis*, 96(3-4):251–281, February 2016.

[37] E. L. Starostin and G. H. M. van der Heijden. Equilibrium Shapes with Stress Localisation for Inextensible Elastic Möbius and Other Strips. *Journal of Elasticity*, 119(1-2):67–112, August 2014.

[38] K. Tosio. *Perturbation Theory for Linear Operators*. Springer Berlin Heidelberg, 1995.

[39] K. Yakubo, Y. Avishai, and D. Cohen. Persistent currents in Möbius strips. *Physical Review B*, 67(12), March 2003.

[40] K. Zahradová. Frame defined by parallel transport for curves in any dimension, 2016.